AIMS Mathematics, 11(4): 9166–9190.
DOI: 10.3934/math.2026378
Received: 23 January 2026
Revised: 19 March 2026
Accepted: 30 March 2026
Published: 02 April 2026

http://www.aimspress.com/journal/Math

Research article

Novel adaptive synchronization criteria of fractional-order fuzzy neural networks with parameter uncertainties and information interactions

Anran Zhou and Hongguang Fan*

College of Computer, Chengdu University, Chengdu 610106, China

* **Correspondence:** Email: fanhongguang@cdu.edu.cn.

Abstract: This research demonstrates a focus on the complete synchronization of fractional-order neural networks with bounded parameter uncertainties and information interactions. The drive-response network models considered in this article contain the operators fuzzy AND, fuzzy OR, and nonlinear interaction modes, which makes the systems in this article more generalized. To achieve complete synchronization tasks, we design a new nonlinear adaptive control scheme. Unlike existing control strategies, the controller incorporates a sign function and a monotonically decreasing function, ensuring the boundedness of the controller even as the error approaches zero, while reducing the conservatism of the control intensity. By virtue of fractional calculus properties and inequality analysis techniques, new synchronization criteria of the concerned drive–response networks are established under the adaptive control schemes. Numerical examples demonstrate the effectiveness of the method proposed in this research.

Keywords: synchronization; sign function; adaptive control; fractional-order; drive-response networks
Mathematics Subject Classification: 26A33

1. Introduction

Over recent decades, neural networks (NNs) have evolved into powerful paradigms for addressing complex, uncertain, and nonlinear problems in artificial intelligence, data science, and other diverse fields [1–3]. Although traditional integer-order NNs excel at learning large-scale data through layered weight adjustments, they often struggle to capture the long-term memory effects in real-world systems [4]. To overcome this limitation, integrating fractional calculus with fuzzy models has garnered considerable interest, leading to the development of fractional-order inpulsive systems [5, 6] and fractional-order fuzzy neural networks (FOFNNs) [7–10]. Fractional calculus, as a generalization of integer-order calculus, offers a rigorous mathematical tool to characterize the memory and hereditary

properties of complex systems [11, 12]. This empowers FOFNNs to model dynamic behaviors with greater precision and flexibility than previous methods [13, 14].

Driven by its unique ability to model uncertain, memory-dependent dynamic systems, the dynamic behaviors of FOFNNs have garnered considerable scholarly interest [15]. Consequently, the synchronization of FOFNNs has become a prominent research focus, with a growing body of literature devoted to its analysis and control. Based on the required convergence time, the synchronization of FOFNNs can be categorized into complete synchronization (CS) [16–18], asymptotic synchronization [19–21], finite-time synchronization (FTS) [22–24], fixed-time synchronization [25–28], quasi-synchronization [29, 30], projective synchronization [31], and more. For example, the CS and FTS of FOFNNs were discussed via two different nonlinear controllers in [16]. In [17], the authors dealt with CS for discrete-time FOFNNs with time-varying delays. A hybrid controller was adopted in [18] to explore the CS of delayed complex-valued FOFNNs.

Traditional control strategies usually assume that feedback parameters are completely known, which tend to suffer from degraded synchronization performance in the presence of actual parameter perturbations. In the study on the CS of FOFNNs presented in [16], the uncertainty of model parameters was not taken into account. The literature [32] studied quasi-projective synchronization and CS of fractional-order complex-valued NNs without considering parameter uncertainty. The FTS issues were addressed in delayed fractional-order complex-valued NNs that incorporate uncertain parameters and fractional difference operators [33]. Nevertheless, fuzzy operators were neglected in the fractional-order models presented in [32,33]. In [34], CS problems of FOFNNs involving uncertain parameters were solved by designing adaptive pinning controllers. In [35], scholars carried out a study on synchronization for discrete-time tempered and competitive FOFNNs in the presence of uncertain parameters and time-varying delays. In [36], a feedback controller was adopted to investigate the FTS of a category of fractional-order delayed fuzzy cellular NNs subject to parameter uncertainties.

In addition, practical neural network systems do not exist in isolation, and there exists interaction information between subnetworks [37]. These inter-network interactions, which may arise from signal transmission, distributed sensing, or coordinated control architectures, substantially influence system dynamics and must be carefully accounted for in both modeling and controller design. Recent studies have increasingly focused on incorporating such interaction effects into synchronization analysis. In [38], the global asymptotic synchronization of FOFNNs with interactions was investigated by designing a hybrid controller. An investigation of fixed-time synchronization was presented in [39], focusing on fractional-order fuzzy cellular NNs with interactions. However, regarding the complete synchronization problem of FOFNNs, existing studies have basically neglected the factor of interactions among systems.

As a crucial dynamic behavior, CS is an important phenomenon in which all neurons eventually converge to a consistent state. In practical scenarios such as multiagent coordination, power network scheduling, and sensor network data fusion, CS ensures the synchronous completion of given tasks by each subsystem, while avoiding task failures caused by asynchronous node operations. However, research on the adaptive CS of FOFNNs with simultaneous consideration of parameter uncertainties and system interactions remains scarce, and this challenging yet novel issue further highlights the significance of the present work. Motivated by the aforementioned discussions, we devote our efforts to investigating the CS of the fractional-order fuzzy neural networks that involve parameter uncertainties and interactions (FOFNNUIs) via adaptive feedback control strategies. The comparison of different

features with existing synchronization results can be seen in Table 1.

Table 1. Comparison of different features with existing synchronization results.

Contents	[17]	[24]	[35]	[39]	Current article
Uncertainties	×	✓	✓	×	✓
Information interactions	×	×	×	✓	✓
Fuzzy operators	✓	×	✓	✓	✓
Bounded controller	✓	×	×	✓	✓

The main highlights of the paper are outlined below:

(i) Given that practical systems are susceptible to uncertainties as well as interactions among systems, this paper addresses the CS issues of fractional-order fuzzy neural networks subject to uncertain parameters and interactions, making the systems more generalized.

(ii) A novel adaptive nonlinear controller, which embeds a sign function and a monotonically decreasing function, is first proposed to address the CS issue for FOFNNUIs. The designed control strategy is capable of guaranteeing controller boundedness as the error tends to zero while properly mitigating the conservatism associated with the control parameters.

(iii) Drawing on the fractional Lyapunov theory and inequality scaling laws, the new CS criteria of FOFNNUIs are obtained.

The remainder of the paper is structured as follows. Section 2 introduces preliminaries and a description of FOFNNUIs. Section 3 presents synchronization criteria of FOFNNUIs. Section 4 provides three illustrative examples together with comparative analyses. Finally, Section 5 concludes the paper.

2. Preliminaries and FOFNNUIs

In this section, some fundamental definitions, helpful lemmas, and a detailed model description of FOFNNUIs are provided.

Definition 1. ([7]) With order λ, the fractional integral of $\varphi(t)$ is defined as:

$$ {}_{t_0}I_t^{\lambda}\varphi(t) = \frac{1}{\Gamma(\lambda)}\int_{t_0}^{t}(t-q)^{\lambda-1}\varphi(q)dq, \quad \lambda > 0, \tag{1} $$

where $\Gamma(\lambda) = \int_0^{+\infty} q^{\lambda-1}e^{-q}dq$.

Definition 2. ([7]) With order λ, the Caputo fractional derivative of function $\varphi(t)$ is defined as:

$$ {}_{t_0}^{c}D_t^{\lambda}\varphi(t) = \frac{1}{\Gamma(1-\lambda)}\int_{t_0}^{t}\frac{\varphi'(q)}{(t-q)^{\lambda}}dq, \quad 0 < \lambda < 1. \tag{2} $$

Definition 3. ([40]) With order λ, the Mittag-Leffler function is defined as:

$$ E_{\lambda}(\theta) = \sum_{\mathrm{m}=0}^{\infty}\frac{\theta^{\mathrm{m}}}{\Gamma(\mathrm{m}\lambda+1)}. \tag{3} $$

Lemma 1. ([41]) Supposing function $\varphi(t) : [t_0, +\infty) \to R_+$ is differentiable, one has

$$ {}_{t_0}^{c}D_t^{\lambda}\varphi^{\nu}(t) \leq \nu\varphi^{\nu-1}(t){}_{t_0}^{c}D_t^{\lambda}\varphi(t), \tag{4} $$

where $0 < \lambda < 1$, and $\nu \geq 1$.

Lemma 2. ([42]) Supposing function $\varphi(t) : [t_0, +\infty) \to R$ is continuous, one has

$$ {}_{t_0}^{c}D_t^{\lambda}\left|\varphi(t)\right| \leq \operatorname{sign}\left(\varphi(t)\right){}_{t_0}^{c}D_t^{\lambda}\varphi(t), \tag{5} $$

where $0 < \lambda < 1$.

Lemma 3. ([43]) Let function $\varphi(t) : [t_0, +\infty) \to R_+$ be differentiable and nondecreasing; then, there is

$$ {}_{t_0}^{c}D_t^{\lambda}\left(\varphi(t) - \iota\right)^2 \leq 2\left(\varphi(t) - \iota\right){}_{t_0}^{c}D_t^{\lambda}\varphi(t), \tag{6} $$

where $t \in [t_0, +\infty)$, $0 < \lambda < 1$, and ι is a constant.

Lemma 4. ([16]) Suppose functions $\varphi_1(t)$ and $\varphi_2(t)$ are non-negative and continuous, which satisfy the following inequality:

$$ {}_{t_0}^{c}D_t^{\lambda}\left(\varphi_1(t) + \varphi_2(t)\right) \leq -\mu_1\varphi_1(t) + \mu_2, \quad 0 < \lambda < 1,\ \mu_1 > 0,\ \mu_2 > 0. \tag{7} $$

Then, one has

$$ \varphi_1(t) \leq \left(\varphi_1\left(t_0\right) + \varphi_2\left(t_0\right) - \frac{\mu_2}{\mu_1}\right)E_{\lambda}\left(-\mu_1\left(t - t_0\right)^{\lambda}\right) + \frac{\mu_2}{\mu_1}, \quad t \geq t_0 + \left(\frac{\Gamma(\lambda)}{\mu_1}\right)^{\frac{1}{1-\lambda}}. \tag{8} $$

Lemma 5. ([44]) When $t \geq t_0$, function $E_{\lambda}\left(\mu_1\left(t - t_0\right)^{\lambda}\right)$ is monotonically nonincreasing and satisfies the inequality $0 \leq E_{\lambda}\left(\mu_1\left(t - t_0\right)^{\lambda}\right) \leq 1$ for $\mu_1 \leq 0$.

We consider a fractional-order fuzzy neural network in the presence of uncertainties and interactions described by

$$ \begin{aligned} {}_{t_0}^{c}D_t^{\lambda}z_{\zeta}(t) =& (-\tilde{c}_{\zeta} + \Delta\tilde{c}_{\zeta}(t))z_{\zeta}(t) + \sum_{\kappa=1}^{\varpi}\left[a_{\zeta\kappa} + \Delta a_{\zeta\kappa}(t)\right]g_{\kappa}(z_{\kappa}(t)) + \bigwedge_{\kappa=1}^{\varpi}\alpha_{\zeta\kappa}g_{\kappa}(z_{\kappa}(t)) \\ &+ \bigvee_{\kappa=1}^{\varpi}\beta_{\zeta\kappa}g_{\kappa}(z_{\kappa}(t)) + I_{\zeta}(t) + \bigwedge_{\kappa=1}^{\varpi}W_{\zeta\kappa}V_{\kappa} + \bigvee_{\kappa=1}^{\varpi}Q_{\zeta\kappa}V_{\kappa} + \xi\sum_{\kappa=1}^{\varpi}\varrho_{\zeta\kappa}h_{\kappa}(r_{\kappa}(t)), \end{aligned} \tag{9} $$

where $\zeta \in N^* = \{1, 2, \cdots, \varpi\}$, $0 < \lambda < 1$, $z_{\zeta}(t)$ signifies the state variable corresponding to the ζth node. $\tilde{c}_{\zeta}$ is positive and denotes the self-feedback coefficient. $a_{\zeta\kappa}$ denotes the feedback template values. The uncertainty parts of $\tilde{c}_{\zeta}$ and $a_{\zeta\kappa}$ are respectively denoted by $\Delta\tilde{c}_{\zeta}(t)$ and $\Delta a_{\zeta\kappa}(t)$, which satisfy $\left|\Delta\tilde{c}_{\zeta}(t)\right| \leq \mathrm{C}_{\zeta}$ and $\left|\Delta a_{\zeta\kappa}(t)\right| \leq A_{\zeta\kappa}$ with $\mathrm{C}_{\zeta} > 0$, $A_{\zeta\kappa} > 0$. $\bigwedge$ and $\bigvee$ stand for the fuzzy AND and fuzzy OR operators, respectively. $\alpha_{\zeta\kappa}$ and $\beta_{\zeta\kappa}$, respectively, denote the fuzzy MIN feedback pattern and fuzzy MAX feedback pattern. $I_{\zeta}(t)$ signifies the external input associated with the ζth neuron. $W_{\zeta\kappa}$ and $Q_{\zeta\kappa}$ stand for fuzzy feed-forward MIN and MAX patterns, respectively. V_{κ} describes the bias of neuron κ. ξ denotes the positive strength of the outer interaction. The structure of the outer interaction is depicted by $\varrho_{\zeta\kappa}$. The interaction function $h_{\kappa}(t)$ is bounded; namely, there exists a positive constant $\overline{H}_{\kappa}$, which makes $|h_{\kappa}(t)| \leq \overline{H}_{\kappa}$ for $\kappa \in N^*$. $g_{\kappa}(t)$ denotes the nonlinear activation function. Functions $g_{\kappa}(t)$ and $h_{\kappa}(t)$ satisfy Assumption 1 below.

Assumption 1. For any real number $\tilde{x}_1$ and $\tilde{x}_2$, there exist positive constants $G_\kappa > 0$ and $H_\kappa > 0$, which makes the following inequality hold, namely,

$$|g_\kappa(\tilde{x}_1) - g_\kappa(\tilde{x}_2)| \leq G_\kappa |\tilde{x}_1 - \tilde{x}_2|, \ |h_\kappa(\tilde{x}_1) - h_\kappa(\tilde{x}_2)| \leq H_\kappa |\tilde{x}_1 - \tilde{x}_2|. \tag{10}$$

Consider the FOFNNUIs described by Formula (11) as the drive network. The response network is constructed as

$$\begin{aligned} {}_{t_0}^{c}D_t^{\lambda} r_\zeta(t) =& (-\tilde{c}_\zeta + \Delta\tilde{c}_\zeta(t))r_\zeta(t) + \sum_{\kappa=1}^{\varpi}\left[a_{\zeta\kappa} + \Delta a_{\zeta\kappa}(t)\right] g_\kappa(r_\kappa(t)) + \bigwedge_{\kappa=1}^{\varpi} \alpha_{\zeta\kappa} g_\kappa(r_\kappa(t)) \\ &+ \bigvee_{\kappa=1}^{\varpi} \beta_{\zeta\kappa} g_\kappa(r_\kappa(t)) + I_\zeta(t) + \bigwedge_{\kappa=1}^{\varpi} W_{\zeta\kappa} V_\kappa + \bigvee_{\kappa=1}^{\varpi} Q_{\zeta\kappa} V_\kappa + U_\zeta(t) + \xi \sum_{\kappa=1}^{\varpi} \overline{\varrho}_{\zeta\kappa} h_\kappa(z_\kappa(t)), \end{aligned} \tag{11}$$

where $U_\zeta(t)$ represents the controller employed to realize synchronization between the drive–response FOFNNUIs. The structure of the outer interaction is depicted by $\overline{\varrho}_{\zeta\kappa}$.

In addition, the following definitions and lemmas are introduced to analyze the synchronization conditions of the drive and response network.

Definition 4. FOFNNUIs (9) and (11) are said to achieve complete synchronization (CS) if the following condition is satisfied for all $\zeta \in N^*$, namely,

$$\lim_{t \to +\infty} \|r_\zeta(t) - z_\zeta(t)\|_2 = 0. \tag{12}$$

Lemma 6. ([13]) For $z_\kappa, r_\kappa \in R$, ζ, κ, and $\varpi \in \mathbb{Z}_+$, the following inequalities hold true, namely,

$$\left| \bigwedge_{\kappa=1}^{\varpi} \alpha_{\zeta\kappa} g_\kappa(z_\kappa) - \bigwedge_{\kappa=1}^{\varpi} \alpha_{\zeta\kappa} g_\kappa(r_\kappa) \right| \leq \sum_{\kappa=1}^{\varpi} \left|\alpha_{\zeta\kappa}\right| |g_\kappa(z_\kappa) - g_\kappa(r_\kappa)| \tag{13}$$

and

$$\left| \bigvee_{\kappa=1}^{\varpi} \beta_{\zeta\kappa} g_\kappa(z_\kappa) - \bigvee_{\kappa=1}^{\varpi} \beta_{\zeta\kappa} g_\kappa(r_k) \right| \leq \sum_{\kappa=1}^{\varpi} \left|\beta_{\zeta\kappa}\right| |g_\kappa(z_\kappa) - g_\kappa(r_\kappa)|. \tag{14}$$

Based on the drive FOFNNUIs (9) and the response FOFNNUIs (11), the error network is defined as

$$\begin{aligned} {}_{t_0}^{c}D_t^{\lambda} e_\zeta(t) =& (-\tilde{c}_\zeta + \Delta\tilde{c}_\zeta(t))e_\zeta(t) + \sum_{\kappa=1}^{\varpi}\left[a_{\zeta\kappa} + \Delta a_{\zeta\kappa}(t)\right] g_\kappa(e_\kappa(t)) + \bigwedge_{\kappa=1}^{\varpi} \alpha_{\zeta\kappa} g_\kappa(e_\kappa(t)) \\ &+ \bigvee_{\kappa=1}^{\varpi} \beta_{\zeta\kappa} g_\kappa(e_\kappa(t)) + U_\zeta(t) + \xi \sum_{\kappa=1}^{\varpi} \overline{\varrho}_{\zeta\kappa} h_\kappa(z_\kappa(t)) - \xi \sum_{\kappa=1}^{\varpi} \varrho_{\zeta\kappa} h_\kappa(r_\kappa(t)), \end{aligned} \tag{15}$$

where $g_\kappa(e_\kappa(t)) = g_\kappa(r_\kappa(t)) - g_\kappa(z_\kappa(t))$.

Remark 1. The CS problem for FOFNNs was explored in [16] using an adaptive control strategy. Different from the models in [16], the FOFNNUIs model presented in this paper takes both the effects of parameter uncertainties and intersystem interactions into account, which are unavoidable in practical applications. Hence, our model exhibits higher generality.

3. Synchronization criteria of FOFNNUIs

This section presents the sufficient conditions that enable FOFNNUIs (9) and (11) to realize complete synchronization. Additionally, the corresponding design scheme for nonlinear controllers is introduced.

Theorem 1. Under Assumption 1, FOFNNUIs (9) and (11) can achieve complete synchronization through the nonlinear adaptive controller

$$U_\zeta(t) = -\frac{\eta_\zeta^2(t)e_\zeta^3(t)}{\eta_\zeta(t)e_\zeta^2(t)+\chi(t)} - \delta sign(e_\zeta(t)),\ {}^{c}_{t_0}D_t^\lambda \eta_\zeta(t) = \theta_\zeta e_\zeta^2(t), \tag{16}$$

where $\chi(t)$ decreases monotonically with the evolution of time satisfying $\chi(t_0) = \tau > 0$ and $\chi(+\infty) \to 0$, $t \geq 0$, $\theta_\zeta > 0$, $\eta_\zeta(t) > 0$, $\delta > \sum_{\kappa=1}^{\varpi} \xi \left|\left(\overline{\varrho}_{\zeta\kappa} - \varrho_{\zeta\kappa}\right)\right| \overline{H}_\kappa$ for $\zeta \in N^*$.

Proof. Construct the following Lyapunov function

$$v_1(t) = v_{11}(t) + v_{12}(t), \tag{17}$$

where $v_{11}(t) = \frac{1}{2}\sum_{\zeta=1}^{\varpi} e_\zeta^2(t)$, $v_{12}(t) = \frac{1}{2}\sum_{\zeta=1}^{\varpi} \frac{1}{\theta_\zeta}(\eta_\zeta(t) - \eta_\zeta^*)^2$. η_ζ^* is a constant and satisfies the following condition:

$$\begin{aligned}\eta_\zeta^* >& \mathrm{C}_\zeta - \tilde{c}_\zeta + \frac{1}{2}\sum_{\kappa=1}^{\varpi}\Big[G_\kappa(|a_{\zeta\kappa}| + A_{\zeta\kappa} + |\alpha_{\zeta\kappa}| + |\beta_{\zeta\kappa}|) + G_\zeta(|a_{\kappa\zeta}| + A_{\kappa\zeta} + |\alpha_{\kappa\zeta}| + |\beta_{\kappa\zeta}|) \\ &+ \xi\varrho_{\zeta\kappa}^* H_\kappa + \xi\varrho_{\kappa\zeta}^* H_\zeta\Big],\end{aligned} \tag{18}$$

where $\varrho_{\zeta\kappa}^* = \min\left\{\left|\varrho_{\zeta\kappa}\right|, \left|\overline{\varrho}_{\zeta\kappa}\right|\right\}$.

Based on Lemma 3, one can get

$$\begin{aligned}{}^{c}_{t_0}D_t^\lambda v_1(t) \leq& \sum_{\zeta=1}^{\varpi} e_\zeta(t){}^{c}_{t_0}D_t^\lambda e_\zeta(t) + \sum_{\zeta=1}^{\varpi}\frac{1}{\theta_\zeta}(\eta_\zeta(t) - \eta_\zeta^*){}^{c}_{t_0}D_t^\lambda \eta_\zeta(t) \\ =& \sum_{\zeta=1}^{\varpi} e_\zeta(t){}^{c}_{t_0}D_t^\lambda e_\zeta(t) + \sum_{\zeta=1}^{\varpi}(\eta_\zeta(t) - \eta_\zeta^*)e_\zeta^2(t) \\ =& \sum_{\zeta=1}^{\varpi} e_\zeta(t)\Big[(-\tilde{c}_\zeta + \Delta\tilde{c}_\zeta(t))e_\zeta(t) + \sum_{\kappa=1}^{\varpi}[a_{\zeta\kappa} + \Delta a_{\zeta\kappa}(t)]g_\kappa(e_\kappa(t)) + \bigwedge_{\kappa=1}^{\varpi}\alpha_{\zeta\kappa}g_\kappa(e_\kappa(t)) \\ &+ \bigvee_{\kappa=1}^{\varpi}\beta_{\zeta\kappa}g_\kappa(e_\kappa(t)) - \frac{\eta_\zeta^2(t)e_\zeta^3(t)}{\eta_\zeta(t)e_\zeta^2(t)+\chi(t)} - \delta sign\Big(e_\zeta(t)\Big) + \xi\sum_{\kappa=1}^{\varpi}\overline{\varrho}_{\zeta\kappa}h_\kappa(z_\kappa(t)) \\ &- \xi\sum_{\kappa=1}^{\varpi}\varrho_{\zeta\kappa}h_\kappa(r_\kappa(t))\Big] + \sum_{\zeta=1}^{\varpi}(\eta_\zeta(t) - \eta_\zeta^*)e_\zeta^2(t).\end{aligned} \tag{19}$$

In light of the boundedness of the parameter uncertainties, it follows that

$$\sum_{\zeta=1}^{\varpi} e_\zeta(t)\Big[-\tilde{c}_\zeta + \Delta\tilde{c}_\zeta(t)\Big]e_\zeta(t) \leq \sum_{\zeta=1}^{\varpi}(-\tilde{c}_\zeta + \mathrm{C}_\zeta)e_\zeta^2(t). \tag{20}$$

Given Assumption 1 and the boundedness of uncertainties, it can be deduced that

$$\begin{aligned}
&\sum_{\zeta=1}^{\varpi}\sum_{\kappa=1}^{\varpi} e_\zeta(t)[a_{\zeta\kappa}+\Delta a_{\zeta\kappa}(t)]g_\kappa(e_\kappa(t)\\
\le&\sum_{\zeta=1}^{\varpi}\sum_{\kappa=1}^{\varpi}\Big[(|a_{\zeta\kappa}|+|\Delta a_{\zeta\kappa}(t)|)|g_\kappa(e_\kappa(t))||e_\zeta(t)|\Big]\\
\le&\sum_{\zeta=1}^{\varpi}\sum_{\kappa=1}^{\varpi}|a_{\zeta\kappa}|G_\kappa|e_\kappa(t)||e_\zeta(t)|+\sum_{\zeta=1}^{\varpi}\sum_{\kappa=1}^{\varpi}|\Delta a_{\zeta\kappa}(t)|G_\kappa|e_\kappa(t)||e_\zeta(t)|\\
\le&\frac{1}{2}\sum_{\zeta=1}^{\varpi}\sum_{\kappa=1}^{\varpi}|a_{\zeta\kappa}|G_\kappa(e_\zeta^2(t)+e_\kappa^2(t))+\frac{1}{2}\sum_{\zeta=1}^{\varpi}\sum_{\kappa=1}^{\varpi}A_{\zeta\kappa}G_\kappa(e_\zeta^2(t)+e_\kappa^2(t))\\
=&\frac{1}{2}\sum_{\zeta=1}^{\varpi}\sum_{\kappa=1}^{\varpi}G_\kappa(|a_{\zeta\kappa}|+A_{\zeta\kappa})e_\zeta^2(t)+\frac{1}{2}\sum_{\zeta=1}^{\varpi}\sum_{\kappa=1}^{\varpi}G_\zeta(|a_{\kappa\zeta}|+A_{\kappa\zeta})e_\zeta^2(t).
\end{aligned}\tag{21}$$

By Lemma 6 and Assumption 1, we derive that

$$\begin{aligned}
&\sum_{\zeta=1}^{\varpi} e_\zeta(t)\left[\bigwedge_{\kappa=1}^{\varpi}\alpha_{\zeta\kappa}g_\kappa(e_\kappa(t))+\bigvee_{\kappa=1}^{\varpi}\beta_{\zeta\kappa}g_\kappa(e_\kappa(t))\right]\\
\le&\sum_{\zeta=1}^{\varpi}|e_\zeta(t)|\sum_{\kappa=1}^{\varpi}|\alpha_{\zeta\kappa}||g_\kappa(e_\kappa(t))|+\sum_{\zeta=1}^{\varpi}|e_\zeta(t)|\sum_{\kappa=1}^{\varpi}|\beta_{\zeta\kappa}||g_\kappa(e_\kappa(t))|\\
\le&\sum_{\zeta=1}^{\varpi}|e_\zeta(t)|\sum_{\kappa=1}^{\varpi}|\alpha_{i\kappa}|G_\kappa|e_\kappa(t)|+\sum_{\zeta=1}^{\varpi}|e_\zeta(t)|\sum_{\kappa=1}^{\varpi}|\beta_{i\kappa}|G_\kappa|e_\kappa(t)|\\
\le&\frac{1}{2}\sum_{\zeta=1}^{\varpi}\sum_{\kappa=1}^{\varpi}|\alpha_{\zeta\kappa}|G_\kappa(e_\zeta^2(t)+e_\kappa^2(t))+\frac{1}{2}\sum_{\zeta=1}^{\varpi}\sum_{\kappa=1}^{\varpi}|\beta_{\zeta\kappa}|G_\kappa(e_\zeta^2(t)+e_\kappa^2(t))\\
=&\frac{1}{2}\sum_{\zeta=1}^{\varpi}\sum_{\kappa=1}^{\varpi}G_\kappa(|\alpha_{\zeta\kappa}|+|\beta_{\zeta\kappa}|)e_\zeta^2(t)+\frac{1}{2}\sum_{\zeta=1}^{\varpi}\sum_{\kappa=1}^{\varpi}G_\zeta(|\alpha_{\kappa\zeta}|+|\beta_{\kappa\zeta}|)e_\zeta^2(t).
\end{aligned}\tag{22}$$

In addition, utilizing the inequality $0 \le (x_1x_2)/(x_1+x_2) \le x_2$ for any $x_1>0$ and $x_2>0$, it can be obtained that

$$\begin{aligned}
&\sum_{\zeta=1}^{\varpi} e_\zeta(t)\left[-\frac{\eta_\zeta^2(t)e_\zeta^3(t)}{\eta_\zeta(t)e_\zeta^2(t)+\chi(t)}-\delta sign(e_\zeta(t))\right]+\sum_{\zeta=1}^{\varpi}(\eta_\zeta(t)-\eta_\zeta^*)e_\zeta^2(t)\\
=&-\sum_{\zeta=1}^{\varpi}\frac{\eta_\zeta^2(t)e_\zeta^4(t)}{\eta_\zeta(t)e_\zeta^2(t)+\chi(t)}-\sum_{\zeta=1}^{\varpi}e_\zeta(t)\delta sign\left(e_\zeta(t)\right)+\sum_{\zeta=1}^{\varpi}(\eta_\zeta(t)-\eta_\zeta^*)e_\zeta^2(t)\\
=&-\sum_{\zeta=1}^{\varpi}\delta|e_\zeta(t)|-\sum_{\zeta=1}^{\varpi}\eta_\zeta^*e_\zeta^2(t)+\sum_{\zeta=1}^{\varpi}\eta_\zeta(t)e_\zeta^2(t)-\sum_{\zeta=1}^{\varpi}\frac{\eta_\zeta^2(t)e_\zeta^4(t)}{\eta_\zeta(t)e_\zeta^2(t)+\chi(t)}\\
=&-\sum_{\zeta=1}^{\varpi}\delta|e_\zeta(t)|-\sum_{\zeta=1}^{\varpi}\eta_\zeta^*e_\zeta^2(t)+\sum_{\zeta=1}^{\varpi}\frac{\eta_\zeta(t)e_\zeta^2(t)\chi(t)}{\eta_\zeta(t)e_\zeta^2(t)+\chi(t)}
\end{aligned}$$

$$\leq -\sum_{\zeta=1}^{\varpi}\delta|e_{\zeta}(t)| - \sum_{\zeta=1}^{\varpi}\eta_{\zeta}^{*}e_{\zeta}^{2}(t) + \sum_{\zeta=1}^{\varpi}\chi(t)$$
$$= -\sum_{\zeta=1}^{\varpi}\delta|e_{\zeta}(t)| - \sum_{\zeta=1}^{\varpi}\eta_{\zeta}^{*}e_{\zeta}^{2}(t) + \varpi\chi(t). \tag{23}$$

By virtue of the scaling of inequalities, Assumption 1, and $|h_{\kappa}(t)| \leq \overline{H}_{\kappa}$, the cross-term from the information interaction is treated as

$$\sum_{\zeta=1}^{\varpi}\sum_{\kappa=1}^{\varpi}\left|\overline{\varrho}_{\zeta\kappa}h_{\kappa}(z_{\kappa}(t)) - \varrho_{\zeta\kappa}h_{\kappa}(r_{\kappa}(t))\right|$$
$$\leq \sum_{\zeta=1}^{\varpi}\sum_{\kappa=1}^{\varpi}[\left|\overline{\varrho}_{\zeta\kappa}h_{\kappa}(z_{\kappa}(t)) - \overline{\varrho}_{\zeta\kappa}h_{\kappa}(r_{\kappa}(t))\right| + |\overline{\varrho}_{\zeta\kappa}h_{\kappa}(r_{\kappa}(t)) - \varrho_{\zeta\kappa}h_{\kappa}(r_{\kappa}(t))|]$$
$$\leq \sum_{\zeta=1}^{\varpi}\sum_{\kappa=1}^{\varpi}[|\overline{\varrho}_{\zeta\kappa}|H_{\kappa}\,|e_{\kappa}(t)| + \left|\overline{\varrho}_{\zeta\kappa} - \varrho_{\zeta\kappa}\right|\overline{H}_{\kappa}]. \tag{24}$$

Alternatively, one can get

$$\sum_{\zeta=1}^{\varpi}\sum_{\kappa=1}^{\varpi}\left|\overline{\varrho}_{\zeta\kappa}h_{\kappa}(z_{\kappa}(t)) - \varrho_{\zeta\kappa}h_{\kappa}(r_{\kappa}(t))\right|$$
$$\leq \sum_{\zeta=1}^{\varpi}\sum_{\kappa=1}^{\varpi}\left[\left|\left(\overline{\varrho}_{\zeta\kappa} - \varrho_{\zeta\kappa}\right)h_{\kappa}(z_{\kappa}(t))\right| + \left|\varrho_{\zeta\kappa}\left(h_{\kappa}(z_{\kappa}(t)) - h_{\kappa}(r_{\kappa}(t))\right)\right|\right]$$
$$\leq \sum_{\zeta=1}^{\varpi}\sum_{\kappa=1}^{\varpi}\left[\left|\overline{\varrho}_{\zeta\kappa} - \varrho_{\zeta\kappa}\right|\overline{H}_{\kappa} + \left|\varrho_{\zeta\kappa}\right|H_{\kappa}\,|e_{\kappa}(t)|\right]. \tag{25}$$

Combining Ineqs (24) and (25), one can obtain

$$\sum_{\zeta=1}^{\varpi}\sum_{\kappa=1}^{\varpi}\left|\overline{\varrho}_{\zeta\kappa}h_{\kappa}(z_{\kappa}(t) - \varrho_{\zeta\kappa}h_{\kappa}(r_{\kappa}(t)\right| \leq \sum_{\zeta=1}^{\varpi}\sum_{\kappa=1}^{\varpi}\left[\left|\overline{\varrho}_{\zeta\kappa} - \varrho_{\zeta\kappa}\right|\overline{H}_{\kappa} + \varrho_{\zeta\kappa}^{*}H_{\kappa}\,|e_{\kappa}(t)|\right], \tag{26}$$

where $\varrho_{\zeta\kappa}^{*} = \min\left\{\left|\varrho_{\zeta\kappa}\right|, \left|\overline{\varrho}_{\zeta\kappa}\right|\right\}$.

Hence, one can deduce that

$$\sum_{\zeta=1}^{\varpi}e_{\zeta}(t)\left[\xi\sum_{\kappa=1}^{\varpi}\overline{\varrho}_{\zeta\kappa}h_{\kappa}(z_{\kappa}(t)) - \xi\sum_{\kappa=1}^{\varpi}\varrho_{\zeta\kappa}h_{\kappa}(r_{\kappa}(t))\right]$$
$$\leq \sum_{\zeta=1}^{\varpi}|e_{\zeta}(t)|\sum_{\kappa=1}^{\varpi}\xi|(\overline{\varrho}_{\zeta\kappa} - \varrho_{\zeta\kappa})|\overline{H}_{\kappa} + \sum_{\zeta=1}^{\varpi}|e_{\zeta}(t)|\sum_{\kappa=1}^{\varpi}\xi\varrho_{\zeta\kappa}^{*}H_{\kappa}|e_{\kappa}(t)|$$
$$\leq \sum_{\zeta=1}^{\varpi}\sum_{\kappa=1}^{\varpi}\xi|(\overline{\varrho}_{\zeta\kappa} - \varrho_{\zeta\kappa})|\overline{H}_{\kappa}|e_{\zeta}(t)| + \frac{1}{2}\sum_{\zeta=1}^{\varpi}\sum_{\kappa=1}^{\varpi}\xi\varrho_{\zeta\kappa}^{*}H_{\kappa}(e_{\zeta}^{2}(t) + e_{\kappa}^{2}(t))$$
$$= \sum_{\zeta=1}^{\varpi}\sum_{\kappa=1}^{\varpi}\xi|(\overline{\varrho}_{\zeta\kappa} - \varrho_{\zeta\kappa})|\overline{H}_{\kappa}|e_{\zeta}(t)| + \frac{1}{2}\sum_{\zeta=1}^{\varpi}\sum_{\kappa=1}^{\varpi}\xi\varrho_{\zeta\kappa}^{*}H_{\kappa}e_{\zeta}^{2}(t) + \frac{1}{2}\sum_{\zeta=1}^{\varpi}\sum_{\kappa=1}^{\varpi}\xi\varrho_{\kappa\zeta}^{*}H_{\zeta}e_{\zeta}^{2}(t). \tag{27}$$

Substituting inequalities (20)–(23) and (27) into (19), it follows that

$$
\begin{aligned}
{}_{t_0}^{c}D_t^{\lambda}v_1(t) \leq & \sum_{\zeta=1}^{\varpi}(-\tilde{c}_\zeta + \mathrm{C}_\zeta)e_\zeta^2(t) + \frac{1}{2}\sum_{\zeta=1}^{\varpi}\sum_{\kappa=1}^{\varpi} G_\kappa(|a_{\zeta\kappa}| + A_{\zeta\kappa})e_\zeta^2(t) \\
& + \frac{1}{2}\sum_{\zeta=1}^{\varpi}\sum_{\kappa=1}^{\varpi} G_\zeta(|a_{\kappa\zeta}| + A_{\kappa\zeta})e_\zeta^2(t) + \frac{1}{2}\sum_{\zeta=1}^{\varpi}\sum_{\kappa=1}^{\varpi} G_k(|\alpha_{\zeta\kappa}| + |\beta_{\zeta\kappa}|)e_\zeta^2(t) \\
& + \frac{1}{2}\sum_{\zeta=1}^{\varpi}\sum_{\kappa=1}^{\varpi} G_\zeta(|\alpha_{\kappa\zeta}| + |\beta_{\kappa\zeta}|)e_\zeta^2(t) - \sum_{i=1}^{\varpi}\delta|e_\zeta(t)| - \sum_{\zeta=1}^{\varpi}\eta_\zeta^* e_\zeta^2(t) + \varpi\chi(t) \\
& + \sum_{\zeta=1}^{\varpi}\sum_{\kappa=1}^{\varpi}\xi|(\overline{\varrho}_{\zeta\kappa} - \varrho_{\zeta\kappa})|\overline{H}_\kappa|e_\zeta(t)| + \frac{1}{2}\sum_{\zeta=1}^{\varpi}\sum_{\kappa=1}^{\varpi}\xi\varrho_{\zeta\kappa}^* H_\kappa e_\zeta^2(t) + \frac{1}{2}\sum_{\zeta=1}^{\varpi}\sum_{\kappa=1}^{\varpi}\xi\varrho_{\kappa\zeta}^* H_\zeta e_\zeta^2(t) \\
= & \frac{1}{2}\sum_{\zeta=1}^{\varpi}\Bigg[\sum_{\kappa=1}^{\varpi}\Big(G_\kappa(|a_{\zeta\kappa}| + A_{\zeta\kappa} + |\alpha_{\zeta\kappa}| + |\beta_{\zeta\kappa}|) + G_\zeta(|a_{\kappa\zeta}| + A_{\kappa\zeta} + |\alpha_{\kappa\zeta}| + |\beta_{\kappa\zeta}|) \\
& + \xi\varrho_{\kappa\zeta}^* H_\zeta + \xi\varrho_{\zeta\kappa}^* H_\kappa\Big) - 2(\tilde{c}_\zeta + \eta_\zeta^* - \mathrm{C}_\zeta)\Bigg]e_\zeta^2(t) + \varpi\chi(t) \\
& - \sum_{\zeta=1}^{\varpi}\left(\delta - \sum_{\kappa=1}^{\varpi}\xi|(\bar{\varrho}_{\zeta\kappa} - \varrho_{\zeta\kappa})|\overline{H}_\kappa\right)|e_\zeta(t)| \\
= & -\gamma\cdot v_{11}(t) + \varpi\chi(t) - \sum_{\zeta=1}^{\varpi}\left(\delta - \sum_{\kappa=1}^{\varpi}\xi\left|\left(\overline{\varrho}_{\zeta\kappa} - \varrho_{\zeta\kappa}\right)\right|\overline{H}_\kappa\right)\left|e_\zeta(t)\right|,
\end{aligned}
\tag{28}
$$

where

$$
\begin{aligned}
\gamma = \min_{\zeta\in N^*}\Bigg\{ & 2(\tilde{c}_\zeta + \eta_\zeta^* - \mathrm{C}_\zeta) - \sum_{\kappa=1}^{\varpi}\Big[G_\kappa(|a_{\zeta\kappa}| + A_{\zeta\kappa} + |\alpha_{\zeta\kappa}| + |\beta_{\zeta\kappa}|) + \xi\varrho_{\zeta\kappa}^* H_\kappa \\
& + G_\zeta(|a_{\kappa\zeta}| + A_{\kappa\zeta} + |\alpha_{\kappa\zeta}| + |\beta_{\kappa\zeta}|) + \xi\varrho_{\kappa\zeta}^* H_\zeta\Big]\Bigg\}.
\end{aligned}
\tag{29}
$$

By virtue of $\chi(+\infty) \to 0$, for any small positive number $\varepsilon > 0$, $\exists t_1 > 0$, when $t \geq t_1$, the inequality $\chi(t) < (\gamma\varepsilon)/\varpi$ holds. Hence, we get

$$
{}_{t_0}^{c}D_t^{\lambda}\left[v_{11}(t) + v_{12}(t)\right] \leq -\gamma\cdot v_{11}(t) + \gamma\cdot\varepsilon, \quad t \geq t_1. \tag{30}
$$

By Lemma 4, one has

$$
v_{11}(t) \leq (v_1(t_0) - \varepsilon)\, E_\lambda\left(-\gamma\cdot(t - t_0)^\lambda\right) + \varepsilon, \tag{31}
$$

where $t \geq \max\left\{t_0 + \left(\frac{\Gamma(\lambda)}{\gamma}\right)^{\frac{1}{1-\lambda}}, t_1\right\}$.

If $v_1(t_0) \leq \varepsilon$, then $v_{11}(t) \leq \varepsilon$. If $v_1(t_0) > \varepsilon$, due to $\lim_{t\to+\infty} E_\lambda\left(-\gamma\cdot(t - t_0)^\lambda\right) = 0$, $\exists t_2 > 0$; when $t \geq t_2$, there is

$$
E_\lambda\left(-\gamma\cdot(t - t_0)^\lambda\right) < \frac{\varepsilon}{(v_1(t_0) - \varepsilon)}. \tag{32}
$$

From Ineqs (31) and (32), it follows that

$$v_{11}(t) < 2\varepsilon, t \geq \max\left\{t_0 + \left(\frac{\Gamma(\lambda)}{\gamma}\right)^{\frac{1}{1-\lambda}}, t_1,\ t_2\right\}, \tag{33}$$

which indicates $\lim_{t\to+\infty} v_{11}(t) = 0$. By virtue of $v_{11}(t) = \frac{1}{2}\sum_{\zeta=1}^{\varpi} e_\zeta^2(t)$, it follows further that $\lim_{t\to+\infty} \left\|e_\zeta(t)\right\|_2 = 0$. Thus, FOFNNUIs (11) and (13) reach complete synchronization under the nonlinear adaptive controller (16). □

Remark 2. Based on the scaling of inequalities and Assumption 1 with $|h_\kappa(t)| \leq \overline{H}_\kappa$, two distinct bounding strategies are employed to handle the cross-term arising from information interaction, as shown in inequalities (24) and (25).

Remark 3. Figure 1 illustrates the nonlinear adaptive control scheme developed for FOFNNUIs (9) and (11). By deploying the adaptive controller (16) in the response system, we ensure that the error between the drive–response FOFNNUIs converges to zero, as defined in Definition 4. The presented controller incorporates two dedicated modules, with each performing a unique function. The first module $-\frac{\eta_\zeta^2(t)e_\zeta^3(t)}{\eta_\zeta(t)e_\zeta^2(t)+\chi(t)}$ serves to markedly lessen the conservative of the overall control magnitude while ensuring that the controller remains bounded. Even when the system is subjected to unexpected disturbances, such as interaction effects between systems, the second module $-\delta sign(e_\zeta(t))$ can still maintain the stability of the system via a control input with amplitude δ. These modules work in synergy, thereby enabling the whole system to fulfill the objective of complete synchronization.

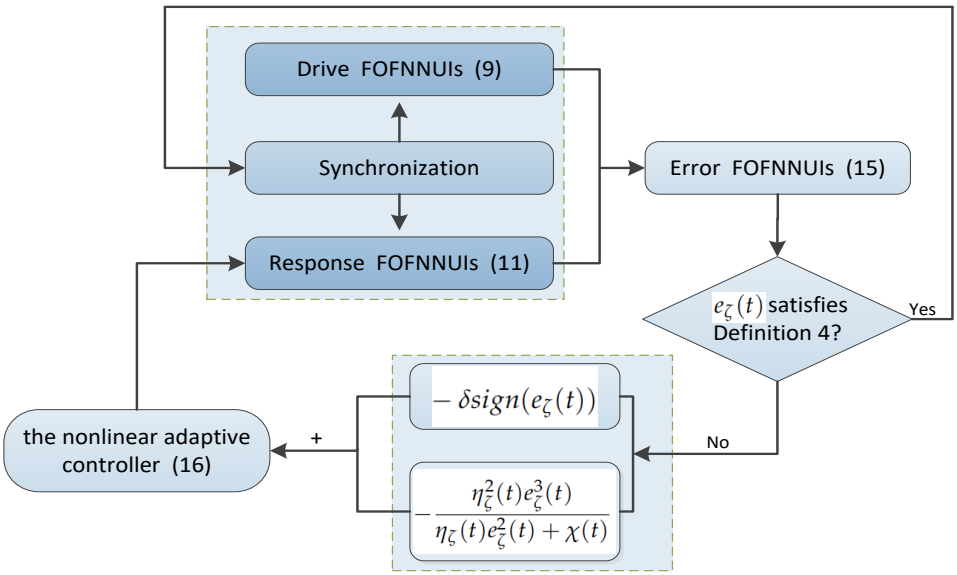

Figure 1. The adaptive control framework for drive–response FOFNNUIs (9) and (11).

Remark 4. The controller in [16], however, has only one module and cannot eliminate the effect of intersystem interactions. Similarly, the controllers in references [17, 18, 34] cannot solve the synchronization task of the drive–response networks in this paper, which is also due to the existence of interaction effects.

Remark 5. Unlike the adaptive linear controllers presented in [32,45], the adaptive nonlinear controller of this study exhibits higher generality, with its control gains $\eta_\zeta(t)$ ($\zeta \in N^*$) being adaptively adjusted and converging to certain constants as the CS of FOFNNUIs is achieved. Compared to the corresponding nonlinear controller with fixed feedback gain [46], the adaptive nonlinear controller proposed in this paper has a lower control cost.

Obviously, if FOFNNUIs (9) and (11) contain no fuzzy logic terms, then $\alpha_{\zeta\kappa} = 0, \beta_{\zeta\kappa} = 0, W_{\zeta\kappa} = 0, Q_{\zeta\kappa} = 0$ for $\zeta, \kappa \in N^*$. Hence, FOFNNUIs (9) and (11) respectively reduce to the following forms, namely,

$$ {}_{t_0}^{c}D_t^{\lambda} z_\zeta(t) = (-\tilde{c}_\zeta + \Delta\tilde{c}_\zeta(t))z_\zeta(t) + \sum_{\kappa=1}^{\varpi}\Big[a_{\zeta\kappa} + \Delta a_{\zeta\kappa}(t)\Big]g_\kappa(z_\kappa(t)) + \xi\sum_{\kappa=1}^{\varpi}\varrho_{\zeta\kappa}h_\kappa(r_\kappa(t)) + I_\zeta(t) \tag{34} $$

and

$$ {}_{t_0}^{c}D_t^{\lambda} r_\zeta(t) = (-\tilde{c}_\zeta + \Delta\tilde{c}_\zeta(t))r_\zeta(t) + \sum_{\kappa=1}^{\varpi}\Big[a_{\zeta\kappa} + \Delta a_{\zeta\kappa}(t)\Big]g_\kappa(r_\kappa(t)) + \xi\sum_{\kappa=1}^{\varpi}\overline{\varrho}_{\zeta\kappa}h_\kappa(z_\kappa(t)) + I_\zeta(t) + U_\zeta(t). \tag{35} $$

Corollary 1. Fractional-order neural networks with uncertainties and interactions (34) and (35) can reach complete synchronization under an adaptive nonlinear controller (16) based on Assumption 1 and the following conditions; that is, $\chi(t)$ exhibits a decreasing trend over time satisfying $\chi(t_0) = \tau > 0$, and $\chi(+\infty) \to 0$, $t \geq 0$, $\theta_\zeta > 0$, $\delta > \sum_{\kappa=1}^{\varpi}\xi\left|\left(\overline{\varrho}_{\zeta\kappa} - \varrho_{\zeta\kappa}\right)\right|\overline{H}_\kappa$ for $\zeta \in N^*$.

Proof. Construct the following Lyapunov function

$$ v_2(t) = v_{21}(t) + v_{22}(t), \tag{36} $$

where $v_{21}(t) = \frac{1}{2}\sum_{\zeta=1}^{\varpi} e_\zeta^2(t)$, $v_{22}(t) = \frac{1}{2}\sum_{\zeta=1}^{\varpi}\frac{1}{\theta_\zeta}(\eta_\zeta(t) - \widetilde{\eta}_\zeta^*)^2$. $\widetilde{\eta}_\zeta^*$ is a constant and satisfies the following condition:

$$ \widetilde{\eta}_\zeta^* > \mathrm{C}_\zeta - \tilde{c}_\zeta + \frac{1}{2}\sum_{\kappa=1}^{\varpi}\Big(G_\kappa\left(\left|a_{\zeta\kappa}\right| + A_{\zeta\kappa}\right) + G_\zeta\left(\left|a_{\kappa\zeta}\right| + A_{\kappa\zeta}\right) + \xi\varrho_{\zeta\kappa}^* H_\kappa + \xi\varrho_{\kappa\zeta}^* H_\zeta\Big), \tag{37} $$

where $\varrho_{\zeta\kappa}^* = \min\left\{\left|\varrho_{\zeta\kappa}\right|, \left|\overline{\varrho}_{\zeta\kappa}\right|\right\}$.

Based on Lemma 3, one can get

$$ \begin{aligned} {}_{t_0}^{c}D_t^{\lambda} v_1(t) &\leq \sum_{\zeta=1}^{\varpi} e_\zeta(t)\,{}_{t_0}^{c}D_t^{\lambda} e_\zeta(t) + \sum_{\zeta=1}^{\varpi}\frac{1}{\theta_\zeta}(\eta_\zeta(t) - \widetilde{\eta}_\zeta^*)\,{}_{t_0}^{c}D_t^{\lambda}\eta_\zeta(t) \\ &= \sum_{\zeta=1}^{\varpi} e_\zeta(t)\,{}_{t_0}^{c}D_t^{\lambda} e_\zeta(t) + \sum_{\zeta=1}^{\varpi}(\eta_\zeta(t) - \widetilde{\eta}_\zeta^*)e_\zeta^2(t) \end{aligned} $$

$$= \sum_{\zeta=1}^{\varpi} e_\zeta(t)\Big[(-\tilde{c}_\zeta + \Delta\tilde{c}_\zeta(t))e_\zeta(t) + \sum_{\kappa=1}^{\varpi}[a_{\zeta\kappa} + \Delta a_{\zeta\kappa}(t)]g_\kappa(e_\kappa(t)) - \frac{\eta_\zeta^2(t)e_\zeta^3(t)}{\eta_\zeta(t)e_\zeta^2(t) + \chi(t)} - \delta sign\Big(e_\zeta(t)\Big) + \xi\sum_{\kappa=1}^{\varpi}\overline{\varrho}_{\zeta\kappa}h_\kappa(z_\kappa(t)) - \xi\sum_{\kappa=1}^{\varpi}\varrho_{\zeta\kappa}h_\kappa(r_\kappa(t))\Big] + \sum_{\zeta=1}^{\varpi}(\eta_\zeta(t) - \widetilde{\eta}_\zeta^*)e_\zeta^2(t). \tag{38}$$

By replacing η_ζ^* with $\widetilde{\eta}_\zeta^*$ in Inequality (23) and substituting Inequalities (20), (21), (23), and (27) into (38), it follows that

$$\begin{aligned}
{}_{t_0}^{c}D_t^{\lambda}v_1(t) \le & \sum_{\zeta=1}^{\varpi}(-\tilde{c}_\zeta + \mathrm{C}_\zeta)e_\zeta^2(t) + \frac{1}{2}\sum_{\zeta=1}^{\varpi}\sum_{\kappa=1}^{\varpi}G_\kappa(|a_{\zeta\kappa}| + A_{\zeta\kappa})e_\zeta^2(t) \\
& + \frac{1}{2}\sum_{\zeta=1}^{\varpi}\sum_{\kappa=1}^{\varpi}G_\zeta(|a_{\kappa\zeta}| + A_{\kappa\zeta})e_\zeta^2(t) - \sum_{i=1}^{\varpi}\delta|e_\zeta(t)| - \sum_{\zeta=1}^{\varpi}\widetilde{\eta}_\zeta^*e_\zeta^2(t) + \varpi\chi(t) \\
& + \sum_{\zeta=1}^{\varpi}\sum_{\kappa=1}^{\varpi}\xi|(\overline{\varrho}_{\zeta\kappa} - \varrho_{\zeta\kappa})|\overline{H}_\kappa|e_\zeta(t)| + \frac{1}{2}\sum_{\zeta=1}^{\varpi}\sum_{\kappa=1}^{\varpi}\xi\varrho_{\zeta\kappa}^*H_\kappa e_\zeta^2(t) + \frac{1}{2}\sum_{\zeta=1}^{\varpi}\sum_{\kappa=1}^{\varpi}\xi\varrho_{\kappa\zeta}^*H_\zeta e_\zeta^2(t) \\
= & \frac{1}{2}\sum_{\zeta=1}^{\varpi}\Big[\sum_{\kappa=1}^{\varpi}\Big(G_\kappa(|a_{\zeta\kappa}| + A_{\zeta\kappa}) + G_\zeta(|a_{\kappa\zeta}| + A_{\kappa\zeta}) + \xi\varrho_{\kappa\zeta}^*H_\zeta + \xi\varrho_{\zeta\kappa}^*H_\kappa\Big) \\
& - 2(\tilde{c}_\zeta + \widetilde{\eta}_\zeta^* - \mathrm{C}_\zeta)\Big]e_\zeta^2(t) + \varpi\chi(t) - \sum_{\zeta=1}^{\varpi}\Big(\delta - \sum_{\kappa=1}^{\varpi}\xi|(\overline{\varrho}_{\zeta\kappa} - \varrho_{\zeta\kappa})|\overline{H}_\kappa\Big)|e_\zeta(t)| \\
= & -\gamma\cdot v_{11}(t) + \varpi\chi(t) - \sum_{\zeta=1}^{\varpi}\Big(\delta - \sum_{\kappa=1}^{\varpi}\xi\Big|\Big(\overline{\varrho}_{\zeta\kappa} - \varrho_{\zeta\kappa}\Big)\Big|\overline{H}_\kappa\Big)\Big|e_\zeta(t)\Big|,
\end{aligned} \tag{39}$$

where

$$\gamma = \min_{\zeta\in N^*}\Big\{2(\tilde{c}_\zeta + \widetilde{\eta}_\zeta^* - \mathrm{C}_\zeta) - \sum_{\kappa=1}^{\varpi}\Big[G_\kappa(|a_{\zeta\kappa}| + A_{\zeta\kappa}) + \xi\varrho_{\zeta\kappa}^*H_\kappa + G_\zeta(|\alpha_{\kappa\zeta}| + A_{\kappa\zeta}) + \xi\varrho_{\kappa\zeta}^*H_\zeta\Big]\Big\}. \tag{40}$$

The remaining proof process is similar to that of Theorem 1, from which it follows that $\lim_{t\to+\infty} v_{21}(t) = 0$. Owing to $v_{21}(t) = \frac{1}{2}\sum_{\zeta=1}^{\varpi}e_\zeta^2(t)$, there is $\lim_{t\to+\infty}\left\|e_\zeta(t)\right\|_2 = 0$. Therefore, NNs (34) and (35) can reach complete synchronization under the nonlinear adaptive controller (16). □

Remark 6. The adaptive nonlinear controller (16), which embeds a sign function and a monotonically decreasing function, is effective to achieve CS for fractional NNs with uncertainties and interactions. This control strategy ensures the boundedness even in the case of error approaching zero, and it lessens the conservatism of the control intensity. The synchronization outcomes obtained in Corollary 1 are built on fractional NNs involving parametric uncertainties and intersystem coupling effects. Thus, the outcome of Corollary 1 can be regarded as a generalized form of studies in [16].

4. Simulation examples

This section provides two examples to verify the effectiveness of the designed controller and derived synchronization criteria.

Example 1. Consider the FOFNNUIs modeled by

$$\begin{aligned} {}_{t_0}^{c}D_t^{0.9} z_\zeta(t) =& (-\tilde{c}_\zeta + \Delta\tilde{c}_\zeta(t)) z_\zeta(t) + \sum_{\kappa=1}^{2} \left[a_{\zeta\kappa} + \Delta a_{\zeta\kappa}(t)\right] g_\kappa(z_\kappa(t)) + \bigwedge_{\kappa=1}^{2} \alpha_{\zeta\kappa} g_\kappa(z_\kappa(t)) \\ &+ \bigvee_{\kappa=1}^{2} \beta_{\zeta\kappa} g_\kappa(z_\kappa(t)) + I_\zeta(t) + \bigwedge_{\kappa=1}^{2} W_{\zeta\kappa} V_\kappa + \bigvee_{\kappa=1}^{2} Q_{\zeta\kappa} V_\kappa + \xi \sum_{\kappa=1}^{2} \varrho_{\zeta\kappa} h_\kappa(r_\kappa(t)), \end{aligned} \tag{41}$$

and

$$\begin{aligned} {}_{t_0}^{c}D_t^{0.9} r_\zeta(t) =& (-\tilde{c}_\zeta + \Delta\tilde{c}_\zeta(t)) r_\zeta(t) + \sum_{\kappa=1}^{2} \left[a_{\zeta\kappa} + \Delta a_{\zeta\kappa}(t)\right] g_\kappa(r_\kappa(t)) + \bigwedge_{\kappa=1}^{2} \alpha_{\zeta\kappa} g_\kappa(r_\kappa(t)) \\ &+ \bigvee_{\kappa=1}^{2} \beta_{\zeta\kappa} g_\kappa(r_\kappa(t)) + I_\zeta(t) + \bigwedge_{\kappa=1}^{2} W_{\zeta\kappa} V_\kappa + \bigvee_{\kappa=1}^{2} Q_{\zeta\kappa} V_\kappa + U_\zeta(t) + \xi \sum_{\kappa=1}^{2} \overline{\varrho}_{\zeta\kappa} h_\kappa(z_\kappa(t)), \end{aligned} \tag{42}$$

where $\zeta = 1, 2$, $\tilde{c}_1 = \tilde{c}_2 = 1, a_{11} = 2.0, a_{12} = -1.2, a_{21} = 1.2, a_{22} = 2.0, \alpha_{11} = 0.15, \alpha_{12} = -0.2, \alpha_{21} = -0.2, \alpha_{22} = 0.15, \beta_{11} = -0.2, \beta_{12} = 0.15, \beta_{21} = 0.2, \beta_{22} = -0.15, \Delta\tilde{c}_1(t) = \Delta a_{1\kappa}(t) = 0.1\sin t, \Delta\tilde{c}_2(t) = \Delta a_{2\kappa}(t) = 0.1\cos t, W_{11} = 0.2, W_{12} = 0.4, W_{21} = 0.4, W_{22} = 0.2, Q_{11} = 0.4, Q_{12} = 0.3, Q_{21} = 0.3, Q_{22} = 0.2, \xi = 1, \varrho_{11} = 1, \varrho_{12} = 2, \varrho_{21} = 2, \varrho_{22} = 1, \bar{\varrho}_{11} = 1, \bar{\varrho}_{12} = 1, \bar{\varrho}_{21} = 1, \bar{\varrho}_{22} = 1$.

Given $g_\kappa(\cdot) = h_\kappa(\cdot) = \tanh(\cdot)$, it is obvious that the upper bound of the function is 1. It can be confirmed that Assumption 1 holds under the condition of $G_\kappa = H_\kappa = 1$. Assume control parameters $\delta = 2$ and $\chi(t) = 0.3\exp(-0.2t)$. Simple calculation shows $\sum_{\kappa=1}^{\varpi} \xi \left|(\overline{\varrho}_{1\kappa} - \varrho_{1\kappa})\right| \overline{H}_\kappa = 1, \sum_{\kappa=1}^{\varpi} \xi \left|(\overline{\varrho}_{2\kappa} - \varrho_{2\kappa})\right| \overline{H}_\kappa = 1$, and one can obtain that the condition of Theorem 1 is satisfied. By virtue of Theorem 1, drive FOFNNUIs (41) and response FOFNNUIs (42) can achieve complete synchronization under the nonlinear adaptive controller (16), as shown in Figure 2. The corresponding error norm curve is shown in Figure 3. The temporal evolution trajectories of $\eta_1(t)$ and $\eta_2(t)$ are depicted in Figures 4 and 5, respectively.

Remark 7. By selecting a series of system parameters, for example, ζ, $\tilde{c}_\zeta$, $a_{\zeta\kappa}$, $\alpha_{\zeta\kappa}$, $\beta_{\zeta\kappa}$, $\Delta\tilde{c}_\zeta(t)$, $\Delta a_{\zeta\kappa}(t)$, $W_{\zeta\kappa}$, $Q_{\zeta\kappa}$, ξ, $\varrho_{\zeta\kappa}$, $\bar{\varrho}_{\zeta\kappa}$, $g_\kappa(t)$, $h_\kappa(t)$, we set their values to satisfy the assumptions of the model. Then, the values of the control parameters are determined, such as δ and $\chi(t)$. Finally, we verify whether the values of the control parameters satisfy sufficient conditions of Theorem 1, for example, $\delta > \sum_{\kappa=1}^{\varpi} \xi |(\overline{\varrho}_{\zeta\kappa} - \varrho_{\zeta\kappa})| \overline{H}_\kappa$ for $\zeta \in N^*$. Both theoretical analysis and numerical simulations verify that the drive FOFNNUIs (41) and response FOFNNUIs (42) can realize CS under the proposed adaptive controller (16).

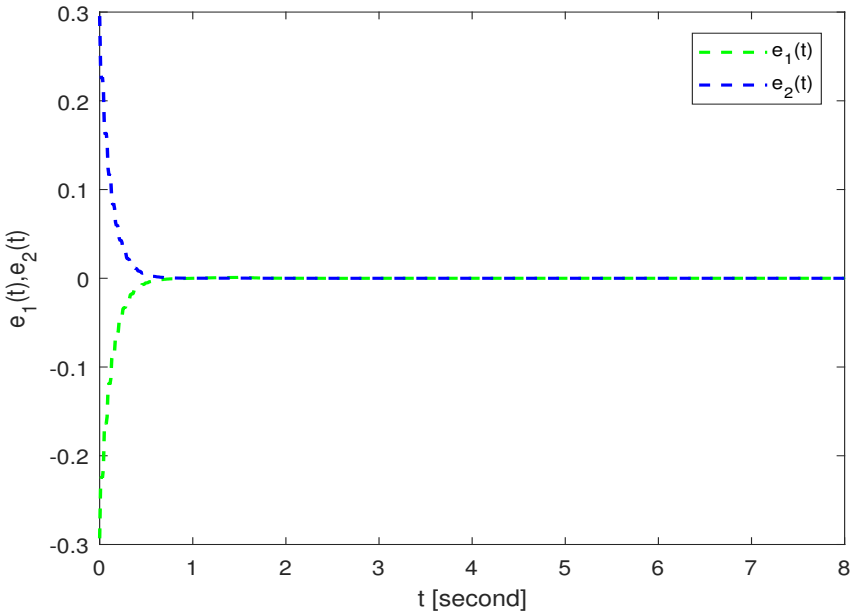

Figure 2. Time evolution of neuron errors $e_1(t)$ and $e_2(t)$ between drive–response FOFNNUIs (41) and (42) in Example 1.

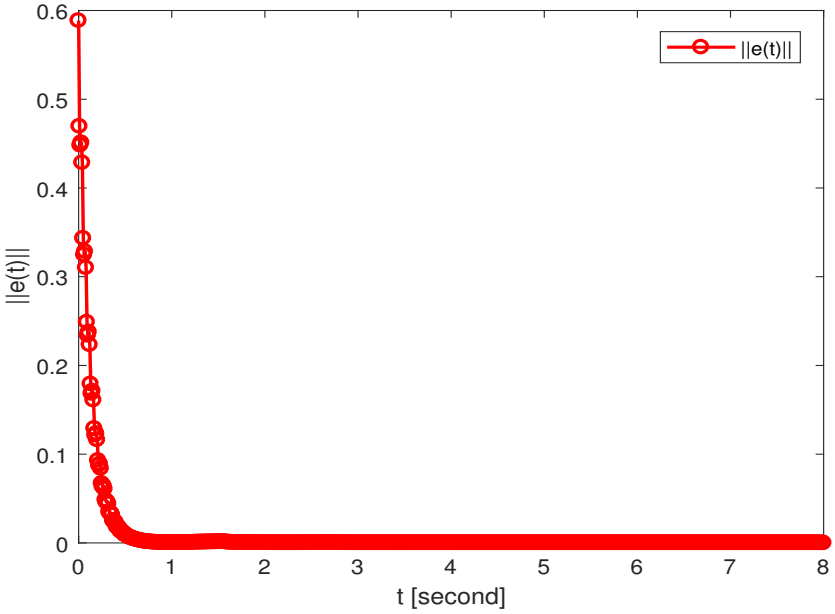

Figure 3. Time evolution of error norm $\|e(t)\|$ between drive–response FOFNNUIs (41) and (42) in Example 1.

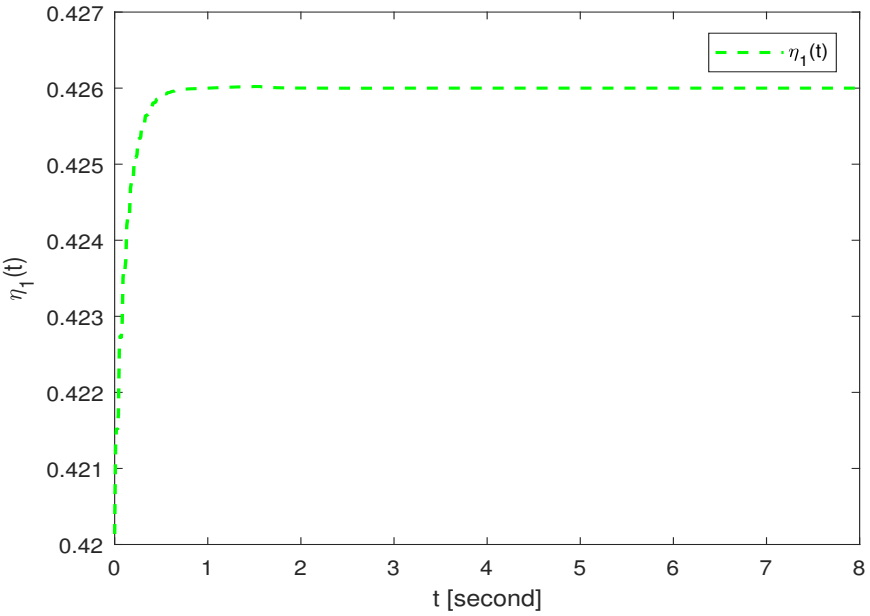

Figure 4. Time evolution of $\eta_1(t)$ between drive–response FOFNNUIs (41) and (42) in Example 1.

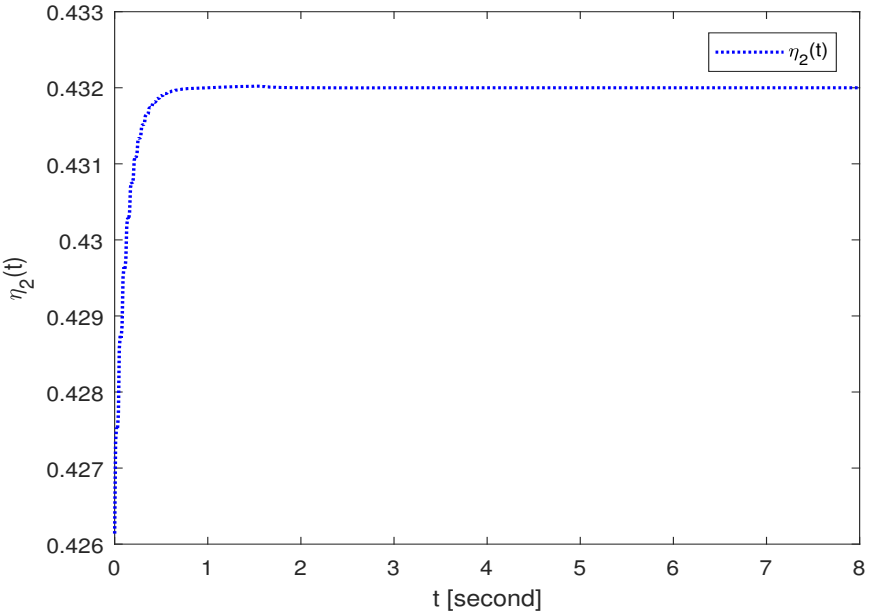

Figure 5. Time evolution of $\eta_2(t)$ between drive–response FOFNNUIs (41) and (42) in Example 1.

Example 2. Take into account the subsequent fractional neural networks that involve parametric uncertainties and information interactions, which are given by

$$ {}_{t_0}^{c}D_t^{0.92} z_\zeta(t) = (-\tilde{c}_\zeta + \Delta\tilde{c}_\zeta(t)) z_\zeta(t) + \sum_{\kappa=1}^{2} \left[a_{\zeta\kappa} + \Delta a_{\zeta\kappa}(t) \right] g_\kappa(z_\kappa(t)) + I_\zeta(t) + \xi \sum_{\kappa=1}^{2} \varrho_{\zeta\kappa} h_\kappa(r_\kappa(t)), \tag{43} $$

and

$$ {}_{t_0}^{c}D_t^{0.92} r_\zeta(t) = (-\tilde{c}_\zeta + \Delta\tilde{c}_\zeta(t)) r_\zeta(t) + \sum_{\kappa=1}^{2} \left[a_{\zeta\kappa} + \Delta a_{\zeta\kappa}(t) \right] g_\kappa(r_\kappa(t)) + I_\zeta(t) + U_\zeta(t) + \xi \sum_{\kappa=1}^{2} \overline{\varrho}_{\zeta\kappa} h_\kappa(z_\kappa(t)), \tag{44} $$

where $\zeta = 1, 2$, $\tilde{c}_1 = 0.2, \tilde{c}_2 = 0.1, a_{11} = -1.2, a_{12} = -2.0, a_{21} = 0.8, a_{22} = -1.4, \Delta\tilde{c}_1(t) = \Delta a_{1\kappa}(t) = 0.1|\sin(t)|, \Delta\tilde{c}_2(t) = \Delta a_{2\kappa}(t) = 0.1(|\sin(t)| + |\cos(t)|), \xi = 1, \varrho_{11} = 1, \varrho_{12} = 1, \varrho_{21} = 1, \varrho_{22} = 1, \bar{\varrho}_{11} = 1, \bar{\varrho}_{12} = 2, \bar{\varrho}_{21} = 2, \bar{\varrho}_{22} = 1$. Letting $g_\kappa(\cdot) = h_\kappa(\cdot) = \tanh(\cdot)$, it is clear that that Assumption 1 holds with $G_\kappa = H_\kappa = 1$.

Set control parameters $\delta = 2.2$ and $\chi(t) = 0.4\exp(-0.3t)$. By simple calculations, we can obtain that $\sum_{\kappa=1}^{\varpi} \xi \left| (\overline{\varrho}_{1\kappa} - \varrho_{1\kappa}) \right| \overline{H}_\kappa = 1, \sum_{\kappa=1}^{\varpi} \xi \left| (\overline{\varrho}_{2\kappa} - \varrho_{2\kappa}) \right| \overline{H}_\kappa = 1$, and the conditions specified in Corollary 1 are met. In accordance with Corollary 1, fractional drive NNs (43) and response NNs (44) without fuzzy terms can achieve complete synchronization under the nonlinear adaptive controller (16). The green dashed line depicts the error evolution curve of the first node, whereas the blue dashed line depicts that of the second node, as illustrated in Figure 6. The corresponding error norm curve is presented in Figure 7, and the time evolution trajectories of $\eta_1(t)$ and $\eta_2(t)$ are presented in Figures 8 and 9, respectively.

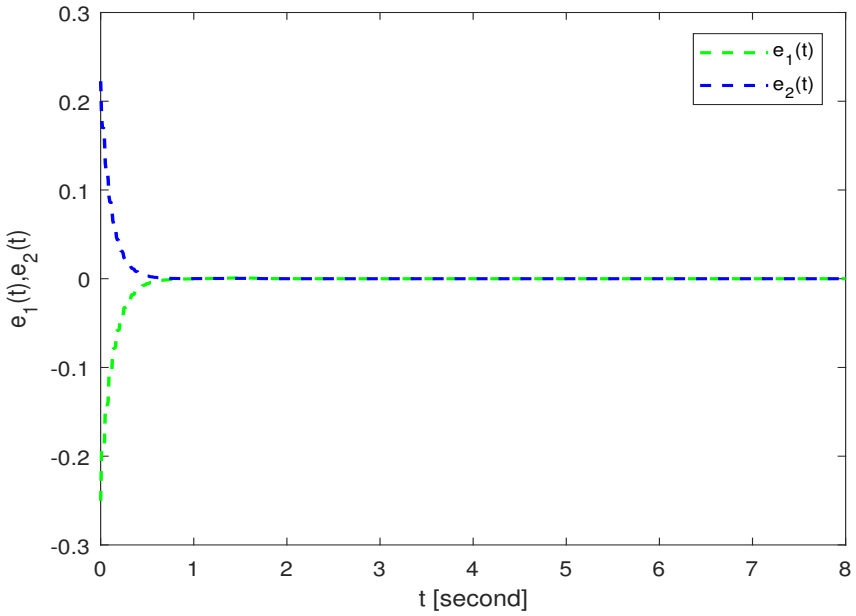

Figure 6. Time evolution of neuron errors $e_1(t)$ and $e_2(t)$ between drive–response networks (43) and (44) in Example 2.

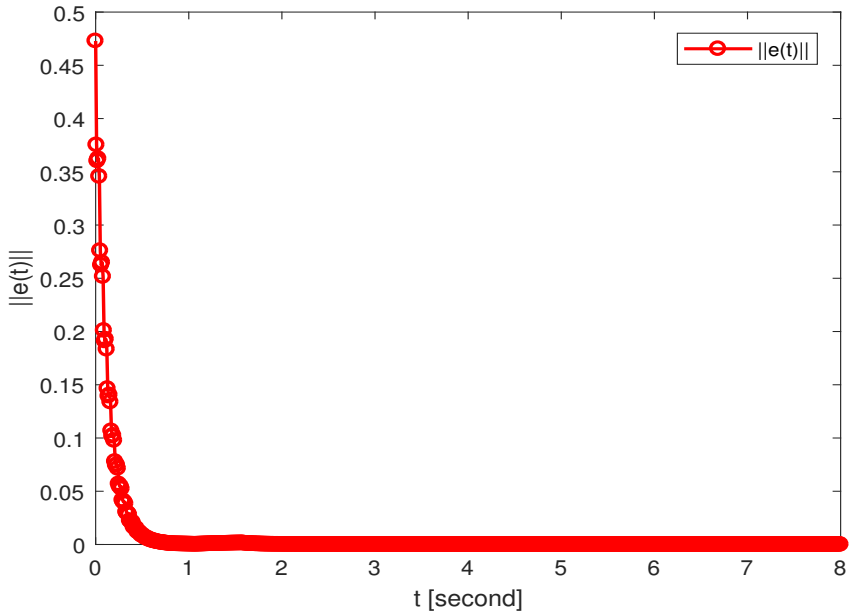

Figure 7. Time evolution of error norm $\|e(t)\|$ between drive–response networks (43) and (44) in Example 2.

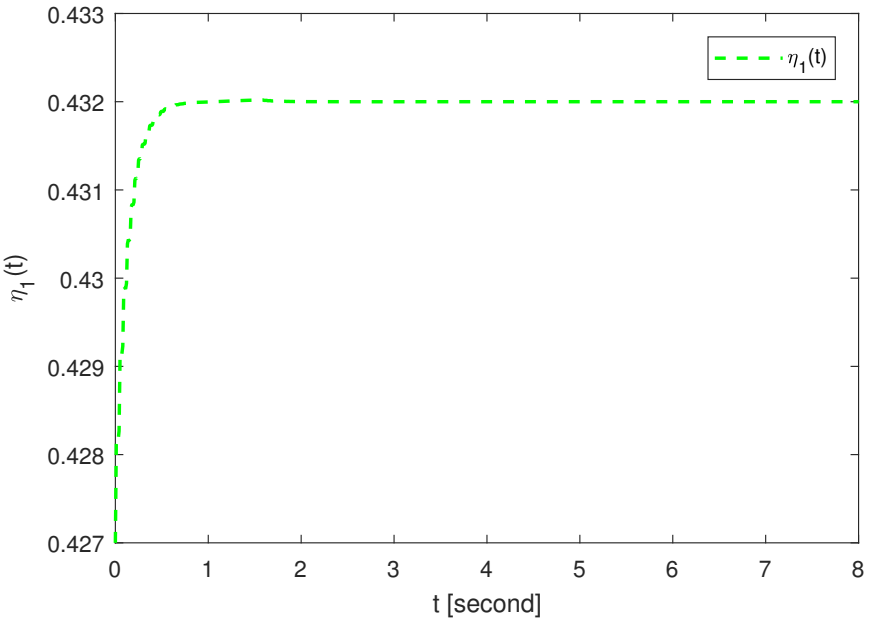

Figure 8. Time evolution of $\eta_1(t)$ between drive–response networks (43) and (44) in Example 2.

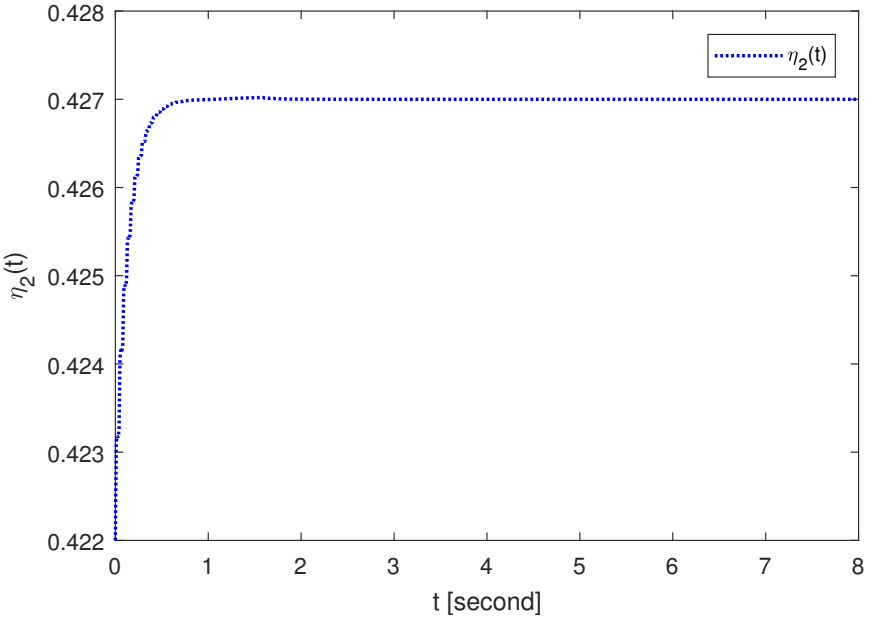

Figure 9. Time evolution of $\eta_2(t)$ between drive–response networks (43) and (44) in Example 2.

Example 3. Consider the FOFNNUIs composed of three nodes presented as follows, which are modeled by

$$\begin{aligned} {}^{c}_{t_0}D^{0.8}_{t} z_\zeta(t) =& (-\tilde{c}_\zeta + \Delta\tilde{c}_\zeta(t))z_\zeta(t) + \sum_{\kappa=1}^{3}\left[a_{\zeta\kappa} + \Delta a_{\zeta\kappa}(t)\right] g_\kappa(z_\kappa(t)) + \bigwedge_{\kappa=1}^{3} \alpha_{\zeta\kappa} g_\kappa(z_\kappa(t)) \\ &+ \bigvee_{\kappa=1}^{3} \beta_{\zeta\kappa} g_\kappa(z_\kappa(t)) + I_\zeta(t) + \bigwedge_{\kappa=1}^{3} W_{\zeta\kappa} V_\kappa + \bigvee_{\kappa=1}^{3} Q_{\zeta\kappa} V_\kappa + \xi \sum_{\kappa=1}^{3} \varrho_{\zeta\kappa} h_\kappa(r_\kappa(t)), \end{aligned} \tag{45}$$

and

$$\begin{aligned} {}^{c}_{t_0}D^{0.8}_{t} r_\zeta(t) =& (-\tilde{c}_\zeta + \Delta\tilde{c}_\zeta(t))r_\zeta(t) + \sum_{\kappa=1}^{3}\left[a_{\zeta\kappa} + \Delta a_{\zeta\kappa}(t)\right] g_\kappa(r_\kappa(t)) + \bigwedge_{\kappa=1}^{3} \alpha_{\zeta\kappa} g_\kappa(r_\kappa(t)) \\ &+ \bigvee_{\kappa=1}^{3} \beta_{\zeta\kappa} g_\kappa(r_\kappa(t)) + I_\zeta(t) + \bigwedge_{\kappa=1}^{3} W_{\zeta\kappa} V_\kappa + \bigvee_{\kappa=1}^{3} Q_{\zeta\kappa} V_\kappa + U_\zeta(t) + \xi \sum_{\kappa=1}^{3} \bar{\varrho}_{\zeta\kappa} h_\kappa(z_\kappa(t)), \end{aligned} \tag{46}$$

where $\zeta = 1, 2, 3$, $\tilde{c}_1 = \tilde{c}_2 = \tilde{c}_3 = 1, a_{11} = 2.0, a_{12} = -1.2, a_{13} = -1.4, a_{21} = 1.2, a_{22} = 2.0, a_{23} = 1.5, a_{31} = 2.2, a_{32} = -1.5, a_{33} = -1.6, \alpha_{11} = 0.15, \alpha_{12} = -0.2, \alpha_{13} = -0.3, \alpha_{21} = -0.2, \alpha_{22} = 0.15, \alpha_{23} = 0.2, \alpha_{31} = -0.3, \alpha_{32} = 0.25, \alpha_{33} = 0.1, \beta_{11} = -0.2, \beta_{12} = 0.15, \beta_{13} = 0.18, \beta_{21} = 0.2, \beta_{22} = -0.15, \beta_{23} = -0.24, \beta_{31} = 0.16, \beta_{32} = 0.25, \beta_{33} = -0.2, \Delta\tilde{c}_1(t) = \Delta a_{1\kappa}(t) = 0.1\sin t, \Delta\tilde{c}_2(t) = \Delta a_{2\kappa}(t) = 0.1\cos t, \Delta\tilde{c}_3(t) = \Delta a_{3\kappa}(t) = -0.15\cos t, W_{11} = 0.2, W_{12} = 0.4, W_{13} = 0.5, W_{21} = 0.4, W_{22} = 0.2, W_{23} = -0.6, W_{31} = 0.1, W_{32} = 0.24, W_{33} = -0.4, Q_{11} = 0.4, Q_{12} = 0.3, Q_{13} = 0.35, Q_{21} = 0.3, Q_{22} = 0.2, Q_{23} = 0.28, Q_{31} = 0.2, Q_{32} = 0.25, Q_{33} = -0.18, \xi = 1, \varrho_{11} = 1, \varrho_{12} = 2, \varrho_{13} = 2.2, \varrho_{21} = 2, \varrho_{22} = 1, \varrho_{23} = 2.4, \varrho_{31} = 1.2, \varrho_{32} = 1.4, \varrho_{33} = 1.8, \bar{\varrho}_{11} = 1, \bar{\varrho}_{12} = 1, \bar{\varrho}_{13} = 1, \bar{\varrho}_{21} = 1, \bar{\varrho}_{22} = 1, \bar{\varrho}_{23} = 1, \bar{\varrho}_{31} = 1, \bar{\varrho}_{32} = 1, \bar{\varrho}_{33} = 1.$

Given $g_\kappa(\cdot) = h_\kappa(\cdot) = \tanh(\cdot)$, it is obvious that the upper bound of the function is 1. It can be confirmed that Assumption 1 holds under the condition of $G_\kappa = H_\kappa = 1$. Set control parameters $\delta = 2$ and $\chi(t) = 0.3\exp(-0.2t)$. Simple calculation shows that $\sum_{\kappa=1}^{\varpi} \xi \left|(\overline{\varrho}_{1\kappa} - \varrho_{1\kappa})\right| \overline{H}_\kappa = 1, \sum_{\kappa=1}^{\varpi} \xi \left|(\overline{\varrho}_{2\kappa} - \varrho_{2\kappa})\right| \overline{H}_\kappa = 1, \sum_{\kappa=1}^{\varpi} \xi \left|(\overline{\varrho}_{3\kappa} - \varrho_{3\kappa})\right| \overline{H}_\kappa = 1$, and one can obtain that the condition of Theorem 1 is satisfied. By virtue of Theorem 1, drive FOFNNUIs (45) and response FOFNNUIs (46) can achieve complete synchronization under the nonlinear adaptive controller (16), as shown in Figure 10. The corresponding error norm curve is shown in Figure 11.

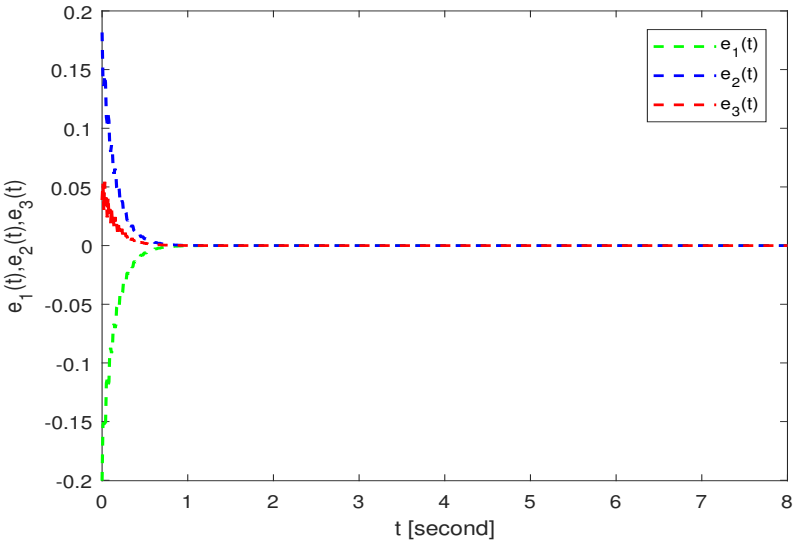

Figure 10. Time evolution of neuron errors $e_1(t)$, $e_2(t)$, and $e_3(t)$ between drive–response networks (45) and (46) in Example 3.

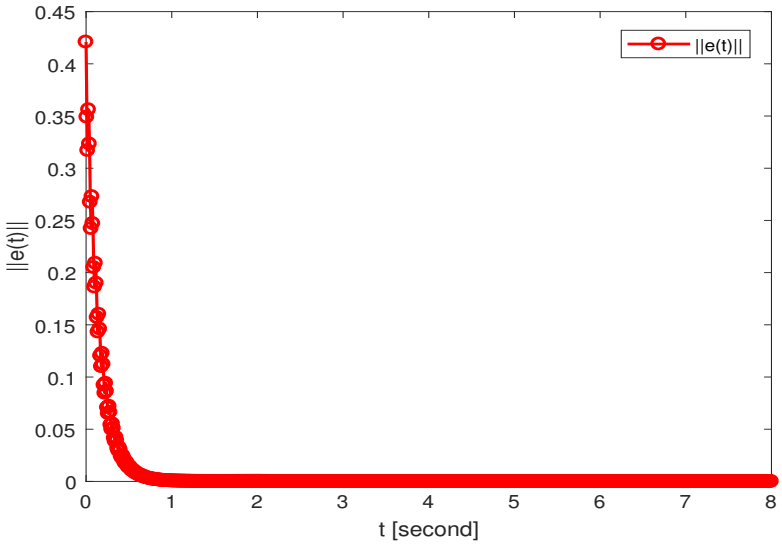

Figure 11. Time evolution of error norm $\|e(t)\|$ between drive–response networks (45) and (46) in Example 3.

Investigating the impact of parameter uncertainty on network synchronization is of significant interest. This study examines how variations in two types of uncertain parameters affect synchronization behavior. To verify the robustness of the proposed control strategy, initial values are randomly selected from the interval $[-0.3, 0.3]$. To begin, the uncertainty parameters $\Delta a_{1k}(t)$ are set to $0.05cost, 0.15cost$, and $0.30cost$, respectively. Then, the uncertain parameters $\Delta\tilde{c}_1(t)$ are configured similarly with the same set of coefficients. As shown in Figures 12 and 13, a larger coefficient in the uncertainty function leads to a longer time required for the network to achieve synchronization. Overall, regardless of the form of parameter uncertainty, the neural network considered in this paper can achieve complete synchronization under appropriately controlled parameters.

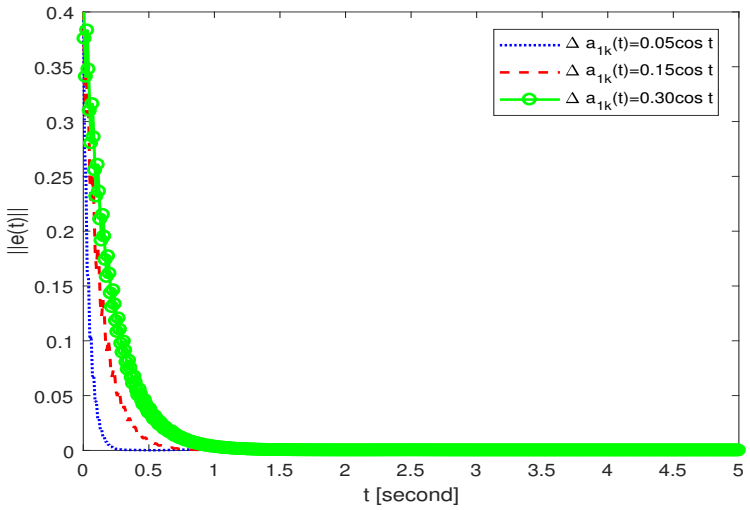

Figure 12. Time evolution of $\|e(t)\|$ between drive–response networks (45) and (46) with different uncertainties $\Delta a_{1k}(t)$.

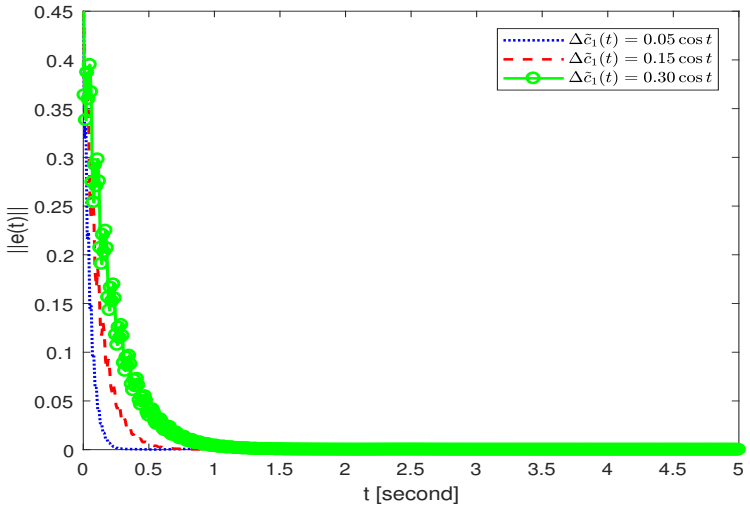

Figure 13. Time evolution of $\|e(t)\|$ between drive–response networks (45) and (46) with different uncertainties $\Delta\tilde{c}_1(t)$.

To assess the efficacy of the adaptive control strategy developed in this article, a comparative study is conducted with the control schemes presented in [9, 22, 26] regarding average convergence time and variances. For impartiality, all comparisons are carried out under the same model parameters without interaction effects. Initial conditions are randomly selected from $[-0.5, 0.5]$, and each control method is executed five times under identical initial settings. As revealed in Table 2, from the perspective of average convergence time, the proposed controller ranks second, and its time variance is the smallest, jointly with that of [26]. The experimental results demonstrate the effectiveness and robustness of the method proposed in this paper.

Table 2. Comparisons of average convergence time and variance with existing results.

Control Methods	**Mean Convergence Time**	**Variance**
Adaptive feedback control scheme in [9]	0.3246	0.021
Adaptive feedback control scheme in [22]	0.3351	0.022
Nonlinear feedback control scheme in [26]	0.3268	0.019
Our adaptive control scheme	0.3255	0.019

5. Conclusions

This study is dedicated to the investigation of CS for fractional-order fuzzy NNs characterized by parameter uncertainties and intersystem coupling effects. To tackle the impacts brought by parametric uncertainties and system interactions, we develop a nonlinear adaptive controller that consists of two components with distinct functions. Based on the constructed Lyapunov function and inequality scaling techniques, sufficient criteria for the CS of FOFNNUIs are derived. In addition, with the proposed control scheme, the boundedness of the controller can be ensured when the error converges to zero, and the conservatism of the control parameters can be alleviated.

In future research, our goal is to design data-driven event-triggered control strategies. Further, we hope to design adaptive event-triggered thresholds to dynamically balance communication resource consumption and control system performance. This method is particularly suitable for scenarios with uncertain model parameters, complex dynamic characteristics, or frequent external disturbances. It can effectively avoid resource waste or performance degradation caused by overly conservative triggering in traditional methods, improve the robustness of control strategies in uncertain environments, and provide key technical support for the real application of fractional-order NNs.

Author contributions

H. Fan: Conceptualization, writing-review and editing; A. Zhou: Methodology, writing-original draft; H. Fan and A. Zhou: Software. All authors have read and agreed to the published version of the manuscript.

Use of Generative-AI tools declaration

The authors declare they have not used Artificial Intelligence (AI) tools in the creation of this article.

Acknowledgments

The first author was partially supported by the Sichuan Provincial Key Laboratory of Cultural and Tourism for Integrated Wine-Tourism and Digital-Intelligent Intangible Cultural Heritage (JLYB12) and the Guangdong Provincial Key Laboratory of Intelligent Information Processing, Shenzhen University (Z1582). The corresponding author was partially supported by the Engineering Research Center for Big Data Application in Private Health Medicine of Fujian Universities, Putian University (MKF202401) and the Fujian Key Laboratory of Financial Information Processing (Putian University)(NO. JXJS202505).

Conflict of interest

All authors declare no conflicts of interest in this paper.

References

1. L. K. Pooja, T. Senthilkumar, Synchronization results for uncertain complex-valued neural networks under delay-dependent flexible impulsive control, *Chaos Soliton. Fract.,* **178** (2024), 114338. https://doi.org/10.1016/j.chaos.2023.114338
2. X. He, X. Li, S. Song, Finite-time stability of state dependent delayed systems and application to coupled neural networks, *Neural Netw.,* **154** (2022), 303–309. http://dx.doi.org/10.1016/j.neunet.2022.07.009
3. A. R. Zhou, C. M. Yang, C. B. Yi, H. G. Fan, New μ-synchronization criteria for nonlinear drive–response complex networks with uncertain inner couplings and variable delays of unknown bounds, *Axioms,* **14** (2025), 161. https://doi.org/10.3390/axioms14030161
4. D. Ding, X. Yao, H. Zhang, Complex projection synchronization of fractional-order complex-valued memristive neural networks with multiple delays, *Neural Process. Lett.,* **51** (2020), 325–345. http://dx.doi.org/10.1007/s11063-019-10093-x
5. Y. Xu, Z. Chen, W. X. Li, Y. B. Wu, Exponential stability of fractional-order fuzzy multilayer networks with short memory and noninstantaneous impulses via intermittent control, *IEEE T. Fuzzy Syst.,* **33** (2025), 1639–1649. http://dx.doi.org/10.1109/TFUZZ.2025.3528975
6. Q. Peng, J. G. Jian, Asymptotic synchronization of second-fractional-order fuzzy neural networks with impulsive effects, *Chaos Soliton. Fract.,* **168** (2023), 113150. https://doi.org/10.1016/j.chaos.2023.113150
7. W. X. Fang, Z. H. Ma, F. X. Li, H. R. Lian, Finite-time stability analysis of fractional-order neural networks with inertial terms and fuzzy logics, *Neurocomputing,* **652** (2025), 131167. https://doi.org/10.1016/j.neucom.2025.131167
8. K. Wu, M. Tang, Z. H. Liu, H. Ren, L. Zhao, Pinning synchronization of multiple fractional-order fuzzy complex-valued delayed spatiotemporal neural networks, *Chaos Soliton. Fract.,* **182** (2024), 114801. https://doi.org/10.1016/j.chaos.2024.114801

9. H. G. Fan, K. B. Shi, Z. Z. Guo, A. R. Zhou, J. Y. Cai, Finite-time synchronization and Mittag–Leffler synchronization for uncertain fractional-order delayed cellular neural networks with fuzzy operators via nonlinear adaptive control, *Fractal Fract.,* **9** (2025), 634. http://dx.doi.org/10.3390/fractalfract9100634
10. J. Xiao, S. Wen, X. Guo, Y. Li, New amplified inequalities and their application on mittag-leffler synchronization problem of fractional-order fuzzy bidirectional associative memory neural networks in octonion-valued field by using a genetic algorithm, *Inform. Sci.,* **727** (2026), 122747. https://doi.org/10.1016/j.ins.2025.122747
11. J. Ran, Y. H. Zhou, H. Pu, Global stability and synchronization of stochastic discrete-time variable-order fractional-order delayed quaternion-valued neural networks, *Math. Comput. Simulat.,* **226** (2024), 413–437. https://doi.org/10.1016/j.matcom.2024.07.017
12. J. Y. Xiao, Y. T. Li, Deep analysis on MLSY for fractional-order higher-dimension-valued neural networks under the action of free quadratic coefficients, *Expert Syst. Appl.,* **298** (2026), 129586. https://doi.org/10.1016/j.eswa.2025.129586
13. J. S. Zhou, G. C. Chen, D. Y. Li, G. D. Zhang, J. H. Hu, Fixed/prescribed-time synchronization of fractional-order fuzzy cellular neural networks with time-varying delays via adaptive control, *Commun. Nonlinear Sci. Numer. Simulat.,* **152** (2026), 109483. https://doi.org/10.1016/j.cnsns.2025.109483
14. G. Narayanan, M. Ali, S. Ahn, Y. Joo, R. Karthikeyan, G. Rajchakit, Fractional impulsive controller design of fractional-order fuzzy systems with average dwell-time strategy and its application to wind energy systems, *Commun. Nonlinear Sci. Numer. Simulat.,* **140** (2025), 108394. http://dx.doi.org/10.1016/j.cnsns.2024.108394
15. Y. Xu, W. X. Liu, Y. B. Wu, W. X. Li, Finite-time synchronization of fractional-order fuzzy time-varying coupled neural networks subject to reaction-diffusion, *IEEE T. Fuzzy Syst.,* **31** (2023), 3423–3432. http://dx.doi.org/10.1109/TFUZZ.2023.3257100
16. H. L. Li, C. Hu, L. Zhang, H. J. Jiang, J. D. Cao, Complete and finite-time synchronization of fractional-order fuzzy neural networks via nonlinear feedback control, *Fuzzy Set. Syst.,* **443** (2022), 50–69. https://doi.org/10.1016/j.fss.2021.11.004
17. H. L. Li, J. D. Cao, C. Hu, L. Zhang, H. J. Jiang, Adaptive control-based synchronization of discrete-time fractional-order fuzzy neural networks with time-varying delays, *Neural Netw.,* **168** (2023), 59–73. https://doi.org/10.1016/j.neunet.2023.09.019
18. J. Li, H. L. Li, J. Yang, L. Zhang, Hybrid control-based synchronization of fractional-order delayed complex-valued fuzzy neural networks, *Comput. Appl. Math.,* **42** (2023), 154. https://doi.org/10.1007/s40314-023-02286-x
19. R. Q. Zhu, Z. Q. Zhang, Asymptotic synchronization of fractional-order fuzzy delayed BAM neural networks by using the integral mean-valued theorem, *Fuzzy Set. Syst.,* **523** (2026), 109637. https://doi.org/10.1016/j.fss.2025.109637
20. F. Lin, Z. Q. Zhang, Global asymptotic synchronization of a class of BAM neural networks with time delays via integrating inequality techniques, *J. Syst. Sci. Complex.,* **33** (2020), 366–382. http://dx.doi.org/10.1007/s11424-019-8121-4

21. X. S. Xiong, Z. Q. Zhang, Asymptotic synchronization of conformable fractional-order neural networks by L' Hopital's rule, *Chaos Soliton. Fract.,* **173** (2023), 113665. http://dx.doi.org/10.1016/j.chaos.2023.113665
22. F. F. Du, J. G. Lu, Adaptive finite-time synchronization of fractional-order delayed fuzzy cellular neural networks, *Fuzzy Set. Syst.,* **466** (2023), 108480. https://doi.org/10.1016/j.fss.2023.02.001
23. H. G. Fan, K. B. Shi, Z. Z. Guo, A. R. Zhou, Finite-time synchronization criteria for Caputo fractional-order uncertain memristive neural networks with fuzzy operators and transmission delay under communication feedback, *Fractal Fract.,* **8** (2024), 619. https://doi.org/10.3390/fractalfract8110619
24. H. L. Li, C. Hu, L. Zhang, H. Jiang, J. D. Cao, Non-separation method-based robust finite-time synchronization of uncertain fractional-order quaternion-valued neural networks, *Appl. Math. Comput.,* **409** (2021), 126377. http://dx.doi.org/10.1016/j.amc.2021.126377
25. M. X. Wang, S. Zhu, W. W. Luo, Z. Zhang, Finite-/Fixed-Time synchronization of coupled memristive neural networks with actuator nonlinearity and applications in secure communication, *IEEE T. Circuits-I.,* **72** (2025), 4334–4345. http://dx.doi.org/10.1109/TCSI.2024.3486586
26. H. G. Fan, H. Wen, K. B. Shi, J. Y. Xiao, New fixed-time synchronization criteria for fractional-order fuzzy cellular neural networks with bounded uncertainties and transmission delays via multi-module control schemes, *Fractal Fract.,* **10** (2026), 91. https://doi.org/10.3390/fractalfract10020091
27. Y. Wan, L. Q. Zhou, Fixed-time synchronization of discontinuous proportional delay inertial neural networks with uncertain parameters, *Inform. Sci.,* **678** (2024), 120931. http://dx.doi.org/10.1016/j.ins.2024.120931
28. P. Kumar, E. A. Assali, Fixed-time synchronization of fractional-order Hopfield neural networks with proportional delays, *Math. Comput. Simulat.,* **240** (2026), 367–380. https://doi.org/10.1016/j.matcom.2025.07.035
29. Z. Tang, J. H. Park, Y. Wang, J. W. Feng, Distributed impulsive quasi-synchronization of Lure networks with proportional delay, *IEEE T. Cybern.,* **49** (2019), 3105–3115. http://dx.doi.org/10.1109/TCYB.2018.2839178
30. H. Y. Yan, Y. H. Qiao, L. J. Duan, J. Miao, New results of quasi-projective synchronization for fractional-order complex-valued neural networks with leakage and discrete delays, *Chaos Soliton. Fract.,* **159** (2022), 112121. http://dx.doi.org/10.1016/j.chaos.2022.112121
31. C. H. Wang, H. L. Li, L. Zhang, C. Hu, J. D. Cao, Synchronization of fractional-order complex-valued T-S fuzzy reaction-diffusion neural networks with time delays and parameter uncertainties, *Commun. Nonlinear Sci. Numer. Simulat.,* **155** (2026), 109594. https://doi.org/10.1016/j.cnsns.2025.109594
32. H. Li, C. Hu, J. Cao, H. Jiang, A. Alsaedi, Quasi-projective and complete synchronization of fractional-order complex-valued neural networks with time delays, *Neural Netw.,* **118** (2019), 102–109. http://dx.doi.org/10.1016/j.neunet.2019.06.008
33. X. B. Chen, R. Y. Ye, H. Zhang, I. Stamova, J. D. Cao, Finite-time synchronization criteria on delayed FOCVNNs with uncertain parameters and difference operator, *J. Franklin Inst.,* **361** (2024), 107017. https://doi.org/10.1016/j.jfranklin.2024.107017

34. R. Y. Ye, X. B. Chen, H. Zhang, J. D. Cao, Novel adaptive pinning synchronization criteria for delayed Caputo-type fuzzy neural networks with uncertain parameters, *Int. J. Control Autom.,* **22** (2024), 2942–2953. http://dx.doi.org/10.1007/s12555-023-0908-3

35. Z. J. Su, H. L. Li, Y. Wang, Y. Q. Chen, J. D. Cao, Synchronization of discrete-time tempered fractional-order fuzzy competitive neural networks with uncertain parameters and time-varying delays, *Commun. Nonlinear Sci.,* **155** (2026), 109603. http://dx.doi.org/10.1016/j.cnsns.2025.109603

36. F. F. Du, J. G. Lu, Finite-time synchronization of fractional-order delayed fuzzy cellar neural networks with parameter uncertainties, *IEEE T. Fuzzy Syst.,* **31** (2023), 1769–1779. https://doi.org/10.1109/Tfuzz.2022.3214070

37. W. G. Sun, Y. Q. Wu, J. Y. Zhang, S. Qin, Inner and outer synchronization between two coupled networks with interactions, *J. Franklin Inst.,* **352** (2015), 3166–3177. http://dx.doi.org/10.1016/j.jfranklin.2014.08.004

38. W. Y. Ma, C. P. Li, Y. J. Wu, Y. Q. Wu, Synchronization of fractional fuzzy cellular neural networks with interactions, *Chaos,* **27** (2017),103106. https://doi.org/10.1063/1.5006194

39. J. Liu, W. J. Deng, S. Q. Sun, K. B. Shi, Novel fixed-time synchronization results of fractional-order fuzzy cellular neural networks with delays and interactions, *AIMS Math.,* **9** (2024), 13245–13264. http://dx.doi.org/10.3934/math.2024646

40. X. N. Yin, H. M. Zhang, H. Zhang, W. W. Zhang, J. D. Cao, New results of global Mittag-Leffler synchronization on Caputo fuzzy delayed inertial neural networks, *Nonlinear Anal.-Model.,* **28** (2023), 613–631. http://dx.doi.org/10.15388/namc.2023.28.31878

41. H. Dai, W. Chen, New power law inequalities for fractional derivative and stability analysis of fractional order systems, *Nonlinear Dyn.,* **87** (2017), 1531–1542. http://dx.doi.org/10.1007/s11071-016-3131-4

42. S. Zhang, Y. Yu, H. Wang, Mittag-Leffler stability of fractional-order Hopfield neural networks, *Nonlinear Anal.-Hybri.,* **16** (2015), 104–121. http://dx.doi.org/10.1016/j.nahs.2014.10.001

43. J. Yu, C. Hu, H. Jiang, Corrigendum to "projective synchronization for fractional neural networks", *Neural Netw.,* **67** (2015), 152–154. https://doi.org/10.1016/j.neunet.2015.02.007

44. D. Basua, S. N. Bora, Nonlinear analysis for Hilfer fractional differential equations, *Franklin Open,* **13** (2025), 100383. https://doi.org/10.1016/j.fraope.2025.100383

45. P. Mani, R. Rajan, L. Shanmugam, Y. Joo, Adaptive control for fractional order induced chaotic fuzzy cellular neural networks and its application to image encryption, *Inform. Sci.,* **491** (2019), 74–89. https://doi.org/10.1016/j.ins.2019.04.007

46. A. M. Zou, Z. G. Hou, M. Tan, Adaptive control of a class of nonlinear pure feedback systems using fuzzy backstepping approach, *IEEE T. Fuzzy Syst.,* **16** (2008), 886–897. http://dx.doi.org/10.1109/tfuzz.2008.917301

AIMS Press